# Carbon emission and export from Ket River, western Siberia

**Artem G. Lim[1], Ivan V. Krickov[1], Sergey N. Vorobyev[1],**

**Mikhail A. Korets[2], Sergey Kopysov[1],**

**Liudmila S. Shirokova[3], Jan Karlsson[4], and Oleg S. Pokrovsky[5*]**

[1]*BIO-GEO-CLIM Laboratory, Tomsk State University, Tomsk, Russia*
[2] *V.N. Sukachev Institute of Forest of the Siberian Branch of Russian Academy of Sciences – separated department of the KSC SB RAS, Krasnoyarsk, 660036, Russia*
[3] *N. Laverov Federal Center for Integrated Arctic Research, Russian Academy of Sciences, Arkhangelsk, Russia*
[4]*Climate Impacts Research Centre (CIRC), Department of Ecology and Environmental Science, Umeå University, Linnaeus väg 6, 901 87 Umeå, Sweden.*
[5] *Geosciences and Environment Toulouse, UMR 5563 CNRS, 14 Avenue Edouard Belin 31400 Toulouse, France*

Key words: $CO_2$, C, emission, boreal, river, export, landscape, Siberia

* email: oleg.pokrovsky@get.omp.eu

## Abstract

Despite recent progress in the understanding of the carbon (C) cycle of Siberian permafrost-affected rivers, spatial and seasonal dynamics of C export and emission from medium-size rivers (50,000 - 300,000 km² watershed area) remain poorly known. Here we studied one of the largest tributaries of the Ob River, the Ket River (watershed = 94,000 km²) which drains through pristine taiga forest of the boreal zone in western Siberian Lowland (WSL). We combined continuous and discrete measurements of carbon dioxide ($CO_2$) concentration using submersible $CO_2$ sensor and floating chamber flux ($FCO_2$), with methane ($CH_4$), organic and inorganic C (DOC and DIC, respectively), particulate organic C and total bacterial concentrations over a 800-km transect of the Ket River main stem and its 26 tributaries during spring flood (May 2019) and 12 tributaries during summer baseflow (end of August – beginning of September 2019). The partial pressure of $CO_2$ ($pCO_2$) was lower and less variable in the main stem (2000 to 2500 µatm) compared to that in tributaries (2000 to 5000 µatm). In the tributaries, the $pCO_2$ was 40 % higher during baseflow compared to spring flood, whereas in the main stem, it did not vary significantly across the seasons. The methane concentration in the main stem and tributaries was a factor of 300 to 1900 (flood period) and 100 to 150 times lower than that of $CO_2$, and ranged from 0.05 to 2.0 µmol $L^{-1}$. The $FCO_2$ ranged from 0.4 to 2.4 g C $m^{-2}$ $d^{-1}$ in the main channel and from 0.5 to 5.0 g C $m^{-2}$ $d^{-1}$ in the tributaries, being the highest during August in tributaries and weakly dependent on season in the main channel. During summer baseflow, the DOC aromaticity, bacterial number, and needleleaf forest coverage of the watershed positively affected $CO_2$ concentrations and fluxes. We hypothesize that relatively low spatial and seasonal variability in $FCO_2$ of the Ket River is due to flat homogeneous landscape (bogs and taiga forest) that results in long water residence times and stable input of allochthonous DOM, which dominate the $FCO_2$. The open water period (May to October) C emission from the fluvial network (main stem and tributaries) of the Ket River was estimated to 127±11 Gg C $y^{-1}$ which is lower than the downstream dissolved and particulate C export during the same period. The estimated fluvial C emissions are highly conservative and contain uncertainties, linked to ignoring hot spots and hot moments of emissions, notably in the floodplain zone. This stresses the need of improving temporal resolution of $FCO_2$ and water coverage across seasons and emphasizes the important role of WSL rivers for release of $CO_2$ to the atmosphere.

## Introduction

Assessment of greenhouse gas (GHG) emission from rivers is crucially important for understanding the C cycle under various climate change scenarios (Campeau and del Giorgio, 2014; Chadburn et al., 2017; Tranvik et al., 2018; Vonk et al., 2019; Vachon et al., 2020). Rivers receive terrestrial C and process and emit a significant share of this C during transit to the sea (Liu et al., 2022). Quantifications of riverine C emissions are sufficiently robust for relatively well studied regions of the world such as the European and N American boreal zone (Dawson et al., 2004; Dinsmore et al., 2013; Wallin et al., 2013; Leith et al., 2015; Zolkos et al., 2019; Hutchins et al., 2020), or Arctic and subarctic rivers of Alaska (Striegl et al., 2012; Crawford et al., 2013; Stackpoole et al., 2017), although subjected to great uncertainty. Despite significant progress in assessing riverine $pCO_2$ in previously under-represented or ignored regions such as lotic systems of Asia (Ran et al., 2015, 2017; Varol and Li, 2017) or South America (Almeida et al., 2017), these studies generally use a combination of pH and alkalinity (DIC) to calculate the $pCO_2$ instead of direct in-situ measurements, alike the studies of global emissions (Raymond et al., 2013; Lauerwald et al., 2015). At the same time, there is a growing number of studies reporting directly measured riverine $pCO_2$ – either discretely (Alin et al. 2011; Borges et al., 2015; Amaral et al. 2018; 2022; Leng et al. 2022), continuously at fixed sites (Crawford et al. 2016a, Schneider et al. 2020; Gómez-Gener et al. 2021a), or along the river flow (Abril et al. 2014; Crawford et al. 2016b; 2017; Borges et al. 2019). However, these studies are limited to tropical and temperate zones of the world, and boreal regions of Western Europe and Northern America, and thus, further continuous and discrete measurements of $CO_2$ concentration and fluxes in rivers from under-represented regions such as Northern Eurasia, and in particular, Siberia, are needed. The on-going interest to Siberia comes from the fact that this region hosts large C stocks in soils and wetlands intersected by extensive river networks that deliver majority of water and C to the Arctic Ocean (Feng et al., 2013).

A few works on Siberian fluvial systems dealt with small (Castro-Morales et al., 2022) and large (Denfeld et al., 2013; Vorobyev et al., 2021) rivers, but these were performed in Eastern Siberia, under continuous permafrost zone. More progress has been achieved in quantification of downstream carbon export by permafrost-affected Great Arctic Rivers of Siberia (Lobbes et al., 2000; Raymond et al., 2007; Cooper et al., 2008; Semiletov et al., 2011; Feng et al., 2013; Griffin et al., 2018; Wild et al., 2019). However, spatial

and seasonal features of C emission from tributaries of large Siberian rivers are still remain poorly known. Existing data on western Siberia (Serikova et al., 2018; Karlsson et al., 2021) suggest that C (predominantly as $CO_2$) emissions from rivers can vary largely over space and time. Such high variations do not allow reliable quantitative assessment of C emission and integrating these values into regional and global C models.

In order to better understand and constrain the magnitude of C emission from Siberian rivers, we studied the Ket River (watershed 94,000 km²), a typical tributary of the Ob River in western Siberia. The Ob river is the largest (in terms of watershed area) Siberian river and drains large pristine territories of taiga forest and bogs. The catchment of Ob includes extensive regions of permafrost but a major part of it (> 80 %) is situated in the permafrost-free zone of which very few data exist on riverine C emissions (Karlsson et al., 2021). The Ket river drains through dense southern taiga forest and abundant wetlands with almost no human activity, thus serving a representative system for understanding C cycling in permafrost-free Siberian rivers. We followed, via a boat routing over the main stem and main tributaries of the river, the in-situ $CO_2$ concentrations combined with discrete sampling for dissolved $CH_4$, DOC, DIC, total bacterial number and particulate organic matter. These measurements were complemented with regular floating chamber measurements of $CO_2$ emission fluxes. We performed these observations during two main open water seasons of the year - the peak of the spring flood and the end of the summer baseflow. Our first objective was to quantify the difference in C concentration and emission during two seasons for the main steam and the tributaries and to relate these differences to main physico-chemical parameters of the water column and physio-geographical parameters (land cover) of the river watersheds. Our second objective was to obtain total C emission flux from the river watershed area and compare it to downstream export yield of dissolved and particulate carbon.

## 2. Study Site, Materials and Methods

### *2.1. Ket River and its tributaries*

The Ket River main stem and its 26 tributaries sampled in this study include watersheds of distinct sizes (catchment area ranged from 94,000 km² at the Ket's mouth to 20 km² of smallest tributary), but rather similar lithology, climate and vegetation (**Fig. 1, Table S1**). The Strahler's order of sampled rivers and stream

ranges from 9 for Ket at its mouth to 2 for the smallest stream. The poorly accessible Ket River basin is fully pristine (50 % forest, 40 % wetlands), and has almost no agricultural and forestry activity. The watershed of Ket has very low population density (0.27 person $km^{-2}$) and lacks road infrastructure due to absence of oil and gas development and production. In this regard, this river can serve as a model for medium size bog-forest rivers of the western Siberia Lowland and results obtained from this watershed can be extrapolated to much larger territory, comprising about 1 million $km^2$ of permafrost-free taiga forest and bog regions of the southern part of WSL.

The mean annual air temperatures (MAAT) is -0.7 ± 0.1 °C and the mean annual precipitation is 520 ± 20 mm $y^{-1}$ in the central part of the basin. The lithology of this part of western Siberian lowland is dominated by Pleistocene silts and sands with carbonate concretions overlayed by quaternary deposits (loesses, fluvial, glacial and lacustrine deposits). The dominant soils are podzols in forest areas and histosols in peat bog regions. Further description of climate, lithology and landscape features of the territory is provided in former studies (Frey and Smith, 2007; Pokrovsky et al., 2015).

The peak of annual discharge in 2019 occurred in the end of May; in August, the discharge was 3 to 5 times smaller (**Fig. 1**). Note that low runoff, lack of relief and highly homogenous landscape coverage of the permafrost-free zone of western Siberia in general and of the Ket River basin in particular provide quite smooth hydrographs of the rivers. In this regard, the spring flood period is extended over 2 months, from the beginning of May to middle of July, whereas summer baseflow includes second half of July, August and September. As a result, similar to previous study of rivers along a 2500 km transect of the WSL territory, the timing of the two sampling campaigns covered approximately 80% of the annual water discharge in the basins (Serikova et al., 2018). From May 18 to May 28, 2019, and from August 30 to September 2, 2019, we started the boat trip in the middle course of the Ket River (Beliy Yar), and moved, first, 475 km upstream the Ket river till its most headwaters, and then moved 834 km downstream till the river mouth, with an average speed of 20 km $h^{-1}$. During summer baseflow, the 4-days trip was shortened by 200 km due to too low water level in the upper reaches of the main stem and some small tributaries. We stopped each 30-50 km along the Ket River and sampled for major hydrochemical parameters, GHG, river suspended matter and total bacterial number of the main stem. We also moved several km upstream of selected tributaries to record $CO_2$

concentrations for at least 1 h and to sample for river hydrochemistry. At several occasions during spring flood, we monitored $CO_2$ concentration and performed chamber measurements in the main stem and tributaries during both day and night time period.

### *2.2. $CO_2$ and $CH_4$ concentrations and $CO_2$ fluxes by floating chambers*

Surface water $CO_2$ concentration was measured continuously, *in-situ* by deploying a portable infrared gas analyzer (IRGA, GMT222 CARBOCAP® probe, Vaisala®; accuracy ± 1.5%) of two ranges (2 000 and 10 000 ppm) as described in previous work of our group on the Lena River (Vorobyev et al., 2021). Sensor preparation was conducted in the lab following the method described by Johnson et al. (2009). The measurement unit (MI70, Vaisala®; accuracy ± 0.2%) was connected to the sensor allowing instantaneous readings of $pCO_2$. The sensors were calibrated in the lab against standard gas mixtures (0, 800, 3 000, 8 000 ppm; linear regression with $R^2 > 0.99$) before and after the field campaign. The sensors' drift was 0.03-0.06% per day and overall error was 4-8% (relative standard deviation, RSD). Following calibration, post-measurement correction of the sensor output induced by changes in water temperature and barometric pressure was done by applying empirically derived coefficients following Johnson et al. (2009). These corrections never exceeded 5% of the measured values. During the cruise, we routinely measured atmospheric $CO_2$ with the probe as a check for its good functioning. Furthermore, we tested two different sensors in several sites of the river transect: a main probe used for continuous measurements and another probe used as a control and never employed for continuous measurements. We did not find any sizable (>10%) difference in measured $CO_2$ concentration between these two probes.

The probe was enclosed within a waterproof and gas-permeable membrane. For this, we used a protective expanded polytetrafluoroethylene (PTFE) sleeve that is highly permeable to $CO_2$ but impermeable to water (Johnson et al., 2009). The sensor was placed into a tube which was submerged 0.5 m below the water surface. A Campbell logger was connected to the system allowing continuous recording of the $CO_2$ concentration, water temperature and pressure every minute. These readings were averaged over 10 minute intervals yielding 732 individual $pCO_2$, water temperature and pressure values. The $CO_2$ concentrations in the Ket River tributaries included between 10 and 20 averaged $pCO_2$ values for each tributary (250 measurements

168 in total) during spring flood period. In addition to continuous *in-situ* $CO_2$ measurements, we estimated $pCO_2$
169 via measured pH and DIC values, using the set of constants typically applied for riverine $pCO_2$ estimation in
170 organic-rich waters (Cai and Wang, 1998; DelDuco and Xu, 2017). The U-test (Mann-Whitney) demonstrated
171 a lack of significant difference in $CO_2$ concentrations measured by Vaissala and calculated from the pH and
172 DIC of the river water.

173 Discrete $CO_2$ fluxes were measured by using two floating $CO_2$ chambers equipped with non-
174 dispersive infrared SenseAir® $CO_2$ loggers (Bastviken et al., 2015), at each of the 7 (spring flood) and 6
175 (summer baseflow) sampling location of the main stem and 26 tributaries following the procedures described
176 elsewhere (Serikova et al., 2019; Krickov et al., 2021). The chambers were not anchored but slowly free-
177 drifted together with the boat, because it is known that anchored chambers can artificially enhance fluxes due
178 to turbulence thus providing erroneous estimates (Lorke et al., 2015). The $CO_2$ accumulation rate inside each
179 chamber was recorded continuously at 300 s interval. We used first 0.5–1 h of measurements for computing
180 $CO_2$ accumulation rate inside each chamber by linear regression.

181 For $CH_4$ analyses, unfiltered water was sampled in 60-mL Serum bottles. For this, the bottles and caps
182 were manually submerged at approx. 30 cm depth from the water surface. The bottles were closed without
183 air bubbles using vinyl stoppers and aluminum caps and immediately poisoned by adding 0.2 mL of saturated
184 $HgCl_2$ via a two-way needle system. The samples were stored approximately one week in the refrigerator
185 before the analyses. In the laboratory, a headspace was created by displacing approximately 40% of water
186 with $N_2$ (99.999%). Two 0.5-mL replicates of the equilibrated headspace were analyzed for their
187 concentrations of $CH_4$, using a Bruker GC-456 gas chromatograph (GC) equipped with flame ionization and
188 thermal conductivity detectors (Serikova et al., 2019; Vorobyev et al., 2021). After every 10 samples, a
189 calibration of the detectors was performed using Air Liquid gas standards (i.e. 145 ppmv). Duplicate injection
190 of the samples showed that results were reproducible within ±5%. The specific gas solubility for $CH_4$
191 (Yamamoto et al., 1976) were used in calculation of the $CH_4$ content in the water. We calculated instantaneous
192 diffusive $CH_4$ fluxes for each of the chambers using chamber-specific gas transfer velocity ($K_T$) and the
193 concentrations of dissolved $CH_4$ in the water and in air-water equilibrium (atm = 1.8 ppm), following the
194 procedure outlined in Serikova et al. (2018), who used the same setup for measurements of GHG emissions

from small and medium-size rivers of the WSL. Note that this setup does not allow measuring the ebullitive $CH_4$ fluxes and thus it is possible that the evasion of $CH_4$, especially in the stagnant zone of the river flow and floodplain in this study is sizably underestimated (i.e., Spawn et al., 2015; Stanley et al., 2016; Villa et al., 2021).

*2.3. Chemical analyses of the river water*

The dissolved oxygen (CellOx 325; accuracy of ±5%), specific conductivity (TetraCon 325; ±1.5%), and water temperature (±0.2 °C) were measured in-situ at 20 cm depth using a WTW 3320 Multimeter. The pH was measured using portable Hanna instrument via combined Schott glass electrode calibrated with standard buffer solutions (4.01, 6.86 and 9.18 at 25°C), with an uncertainty of 0.01 pH units. The temperature of buffer solutions was within ± 2°C of that of the river water. The water was sampled in pre-cleaned polypropylene bottle from 20-30 cm depth in the middle of the river and immediately filtered through disposable single-use sterile Sartorius filter units (0.45 µm pore size). The first 50 mL of filtrate was discarded. The DOC and Dissolved Inorganic Carbon (DIC) were determined by a Shimadzu TOC-VSCN Analyzer (Kyoto, Japan) with an uncertainty of 3% and a detection limit of 0.1 mg/L. Blanks of MilliQ water passed through the filters demonstrated negligible release of DOC from the filter material. The SUVA was measured via ultraviolet absorbance at 254 nm using a 10-mm quartz cuvette on a Bruker CARY-50 UV-VIS spectrophotometer.

The concentration of C and N in suspended material (Particulate Organic Carbon and Nitrogen (POC and PON, respectively)) was determined via filtration of 1 to 2 L of freshly collected river water (at the river bank or in the boat) with pre-weighted GFF filters (47 mm, 0.45 µm) and Nalgene 250-mL polystyrene filtration units using a Mityvac® manual vacuum pump. Particulate C and N were measured using catalytic combustion with Cu-O at 900°C with an uncertainty of ≤ 0.5% using Thermo Flash 2000 CN Analyzer at EcoLab, Toulouse. The samples were analyzed before and after 1:1 HCl treatment to distinguish between total and inorganic C; however the ratio of $C_{organic}$ : $C_{carbonate}$ in the river suspended matter (RSM) was always above 20 and the contribution of carbonate C to total C in the RSM was equal in average 0.3±0.3% (2 s.d., n = 30).

Total microbial cell concentration was measured after sample fixation in glutaraldehyde, by a flow cytometry (Guava® EasyCyteTM systems, Merck). Cells were stained using 1 µL of a 10 times diluted SYBR GREEN solution (10000x, Merck), added to 250 µL of each sample before analysis. Particles were identified as cells based on green fluorescence and forward scatter (Marie et al., 2001).

*2.4. Riverine carbon export flux by the Ket catchment*

The C export flux over active (unfrozen) period (May to October) from the Ket basin was calculated based on monthly-averaged discharge at the river mouth in 2019 available from Russian Hydrological Survey and DOC, DIC and POC concentrations measured in the low reaches of the Ket River in this study (see hydrograph in **Fig. 1**). Riverine element fluxes should be usually estimated using a LOADEST method (Holmes et al., 2012) from calculated daily element loads. The latter typically obtained from a calibration regression, applied to daily discharge. This calibration regression can be constructed from time series of paired streamflow and measured element concentration data for sufficient period of the year. In our previous works in this and other similar boreal regions, we demonstrated that this method provides reasonable (within 10 to 30 %) agreement with monthly export fluxes calculated by multiplying mean monthly discharge by mean monthly concentration (Chupakov et al., 2020; Pokrovsky et al., 2022; Vorobyev et al., 2019). Given that the intrinsic uncertainties on mean monthly discharge are also between 10 and 20 % (see discussion for the WSL rivers in Pokrovsky et al., 2020), in this study, for open-water period export flux calculation, we used DOC, DIC and POC concentrations measured during spring flood (for May and June period) and baseflow (for August, September and October period). For the month of July, we used the mean concentrations of end of May and August-September which is in accord with seasonal discharge pattern of the Ket River. Note that the contribution of non-studied October month to total open water period water flux is < 10 % and thus cannot provide sizable uncertainties

249 *2.5. Landscape parameters and water surface area of the Ket River basin*

250 The physio-geographical characteristics of the 26 Ket tributaries and the 7 points of the Ket main stem
251 (**Table S1, Fig. S1**) were determined by applying available digital elevation model (DEM GMTED2010),
252 soil, vegetation and lithological maps. The landscape parameters were typified using TerraNorte Database of
253 Land Cover of Russia (Bartalev et al., 2020; http://terranorte.iki.rssi.ru). This included various type of forest
254 (evergreen, deciduous, needleleaf/broadleaf), grassland, tundra, wetlands, water bodies and riparian zones.
255 Note that the land cover data correspond to the whole catchment area upstream of the sampling point. The
256 climate parameters the watershed were obtained from CRU grids data (1950-2016) (Harris et al., 2014) and
257 NCSCD data (Hugelius et al., 2013), respectively. The biomass was obtained from BIOMASAR2 dataset in
258 raster format with spatial resolution of 1 x 1 km (Santoro et al., 2010). The soil OC content was taken from
259 the Northern Circumpolar Soil Carbon Database (NCSCD). The original NCSCD dataset produced in GIS
260 vector format corresponding to 1:1,000,000 scale of topographic map. It could be rasterized to 1 x 1 km pixel
261 resolution. The lithology layer was taken from GIS version of Geological map of the Russian Federation
262 (scale 1:5,000,000, http://www.geolkarta.ru/). We quantified river water surface area using the global SDG
263 database with 30 $m^2$ resolution (Pekel et al., 2016) including both seasonal and permanent water for the open
264 water period of 2019 and for the multiannual average (reference period 2000-2004). We also used a more
265 recent GRWL Mask Database which incorporates first order temporary non-active streams (Allen and
266 Pavelsky, 2018).
267
268 *2.6. Data analysis*
269 Carbon concentrations and fluxes for all dataset were tested for normality using a Shapiro-Wilk test.
270 In case if the data were not normally distributed, we used non-parametric statistics. Comparisons of GHG
271 parameters in the main stem and tributaries during two sampling seasons were conducted using a non-
272 parametric Mann Whitney test at a significance level of 0.05. For comparison of unpaired data, a non-
273 parametric H-criterion Kruskal-Wallis test was used to reveal the differences between different study sites.
274 The Pearson rank order correlation coefficient ($p < 0.05$) was used to determine the relationship between $CO_2$
275 concentrations and emission fluxes and main landscape parameters of the Ket River tributaries, as well as

other potential drivers such as pH, $O_2$, water temperature, specific conductivity, DOC, DIC, particulate carbon and nitrogen, and total bacterial number.

Further identification of C pattern drivers in river waters included a Principal Component Analysis which allowed to test the effect of various hydrochemical and landscape parameters on $CO_2$ and $CH_4$ concentrations and $CO_2$ emissions. In addition to PCA, a Redundancy analysis (RDA) was used to extract and summarize the variation in C pattern that can be explained by a set of explanatory variables (environmental, climatic and hydrochemical factors). The RDA combines a PCA and multiple regression analysis and it was run in XLSTAT is a statistical software that works as an add-on to Excel.

## 3. Results

### *3.1. Greenhouse gases and dissolved and particulate C*

The main hydrochemical parameters and greenhouse gases concentration and exchange fluxes of the Ket River and its tributaries are listed in **Table 1** and primary data are provided in **Table S2** of the Supplement. Continuous $pCO_2$ measurements in the main stem during the spring (764 individual data points over the full distance of the boat route (834 km) demonstrated a lack of systematic change in $CO_2$ concentration from headwaters to the mouth. The $CO_2$ concentration in tributaries was generally higher than that in the main stem. As a result, the $pCO_2$ changed by a factor of 1.5 to 2 when tributaries with high $CO_2$ concentrations join the main stem (**Fig. 2 A**). There were strong but non-systematic variations in $CO_2$ concentration in the tributaries during the summer (**Fig. 2 C**). The $CH_4$ concentration (**Table 1 and Fig. S2 A, B**) was low in the Ket River (around 0.17 and 0.86 µmol $L^{-1}$ in May and August, respectively) and in the tributaries (range 0.09 to 2.6 µmol $L^{-1}$, 2 to 3 times higher values during the baseflow). These values are generally higher than the range of $CH_4$ concentration in large Siberian Rivers such as Lena (0.03 to 0.199 µmol $L^{-1}$, Bussman, 2013; Vorobyev et al., 2021) but consistent with concentrations in surface layers of East Siberian ponds (0.6-2.4 µmol $L^{-1}$, Rehder et al., 2021). In the Ket River main stem and tributaries, the $CH_4$ concentrations are 300-2000 and 100-150 times lower than those of $CO_2$ during spring and summer,

302 respectively, and ranged from 0.05 to 2.0 µmol $L^{-1}$. Consequently, diffuse $CH_4$ emissions (**Table 1, Fig. S2**
303 **C, D)** constituted 0.1 to 0.5% of total C emissions and are not discussed in further detail.

304 During spring flood, $CO_2$ fluxes ranged from 0.26 to 3.2 g C $m^{-2}$ $d^{-1}$ in the main stem and tributaries
305 (**Table 1; Fig. 2 B**). During baseflow, the flux in the tributaries varied from 0.37 to 7.4 g C $m^{-2}$ $d^{-1}$ and was a
306 factor of 2 to 3 higher than that in the main stem (**Fig. 2 D; Table 1**). The $CO_2$ concentration in the river
307 water and gas transfer velocity assessed from discrete measurements by floating chambers ($K_T$ = 0.08-1.83
308 m $d^{-1}$ in the main stem; 0.2-1.86 m $d^{-1}$ in the tributaries, **Table 1**) allowed for calculation of the continuous
309 $CO_2$ fluxes (**Fig. 2 B**). For this, we used an average value of $K_T$ measured between two chamber sites
310 (separated by a distance of 50 to 100 km) to calculate the $FCO_2$ from in-situ measured $pCO_2$ in the river
311 section between these two sites.

312 The DIC concentration increased 5 to 10 times between the spring (2.4 to 2.8 mg $L^{-1}$) and summer
313 baseflow (18 to 20 mg $L^{-1}$) and the pH increased by 0.5-0.7 units between spring freshet and summer baseflow
314 (**Fig. 3** and **Fig. S3 A, B** of the Supplement). The DOC concentration ranged from 18 to 25 mg $L^{-1}$ during
315 flood and from 15 to 18 mg $L^{-1}$ during baseflow (**Fig. 3**). There was no systematic variations in DOC
316 concentration over the 834 km of the main stem (20.7 ± 3.6 and 15.0 ± 1.4 mg $L^{-1}$ in May and August,
317 respectively); however, it was slightly higher and more variable in the tributaries (22.0± 4.0 and 16.5 ± 7.4
318 mg $L^{-1}$, **Fig. S3 C, D)**. The $SUVA_{254}$ remained highly stable throughout the seasons for both the tributaries
319 and the main stem (range from 4.2 to 4.9 L mg $C^{-1}$ $m^{-1}$, **Table 1**). The POC was 3 times higher during baseflow
320 compared to spring and ranged from 2 to 10 mg $L^{-1}$ (**Fig. 3** and **Fig. S3 E, F**). The total bacterial number
321 ranged from $5.0 \times 10^5$ to $8.7 \times 10^5$ cells $mL^{-1}$ for the main stem and tributaries without significant ($p > 0.05$)
322 seasonal variation (**Fig. 3** and **S3 G, H**).

323

324 *3.2. Diurnal and spatial variation in $CO_2$ concentration and flux*

325 The diel (day/night) measurements of $CO_2$ concentrations have been performed on six tributaries of
326 the Ket River during the spring flood period (**Fig. 4**). In two of them (Sochur ad Lopatka), we measured both
327 $CO_2$ concentration and $CO_2$ fluxes via floating chambers. Continuous $CO_2$ concentrations over 10-38 h
328 exhibited a variation between 5 and 25% of the average value. Only in the case of a small tributary

Segondenka (**Fig. 4 E**), when we measured $CO_2$ over 38 h, there was a local maximum in concentration between 6 and 7 pm during the first and second day of monitoring, without any significant link to the water temperature. The deviation of $FCO_2$ from the average value over the period of observation in two tributaries (**Fig. 4 A, B**) did not exceed 20%, without any detectable difference between day and night period.

The spatial variation in $pCO_2$ and $FCO_2$ were tested during spring time in the flood zone of the Ket River middle course, where the flood zone was connected to the main channel. Regardless of the distance from the main stem and the size of the water body, the variation in $pCO_2$ and chamber-based fluxes were within 30% of the values measured in the main stem. This suggests that the main stem parameters can be used for upscaling the C emissions to the overall flood plain during May, provided that the water bodies are connected to the rivers. Further tests of spatial variation were performed on selected small tributaries, when we moved 8 to 16 km upstream towards the headwaters and monitored the $CO_2$ concentration in the river water. There was no sizable trend in $CO_2$ concentration over several km length of the tributary, consistent with small fluctuations over the hundred km-scale of the main stem (**Fig. S4 A**). Altogether, rather minor spatial and diel variations in both $CO_2$ concentration and emission fluxes support the chosen sampling strategy and allow reliable extrapolation of obtained results to full surface of lotic waters of the Ket River basin, during open water period.

*3.3. Impact of water chemistry and catchment characteristics on $CO_2$ concentrations and emissions*

There were generally no strong correlations between $CO_2$ and $CH_4$ and the main parameters of the water column (DOC, DIC, POC, TBC and SUVA (**Table 2**). The $CO_2$ concentration negatively correlated with $O_2$ concentration ($R_{Pearson} = -0.68$, $p < 0.05$) and $FCO_2$ positively correlated with $SUVA_{254}$ ($R = 0.34$, $p < 0.05$), **Fig. 5 A, B**. Other hydrochemical characteristics of the water column did not impact $CO_2$ and $CH_4$ concentration and $CO_2$ flux. During spring flood, there was no positive correlation between $FCO_2$ of the river water and various hydrochemical characteristics. During the summer baseflow, there were positive correlations between $CO_2$ concentration or flux and SUVA and total bacterial number (**Table 2**).

There was a decrease in $pCO_2$ with an increase in the stream order **(Fig. S5 A**), consistent with negative correlation between $pCO_2$ and $S_{watershed}$ during the spring (**Table 2**). However, neither $FCO_2$ nor gas

transfer coefficient exhibited significant link to the stream order (**Fig. S5 B, C**) or the watershed surface area (**Table 2**). Among different landscape factors, only deciduous light needleleaf forest (larch trees) exhibited significant ($p < 0.01$) positive correlations ($0.6 \leq R_{Pearson} \leq 0.7$) with $CO_2$ concentration and flux of the Ket River main stem and tributaries, detectable only during the summer baseflow period (**Fig. 5 C**). The peatland and bogs at the watershed exhibited only weak, although positive ($0.2 < R_{Pearson} < 0.4$), correlation with $pCO_2$ and $FCO_2$ (**Table 2**). The other potentially important landscape factors of the river watershed (type of forest, riparian and total aboveground vegetation, recent burns, water bodies) did not significantly impact the $CO_2$ and $CH_4$ concentration and measured $CO_2$ fluxes in the Ket River basin (**Table 2**). The mean annual precipitation (MAP) at the watershed positively correlated with $pCO_2$ and $FCO_2$ during the baseflow (**Fig. 5 D**).

Principal Component Analysis (PCA) demonstrated a general lack of control of physico-chemical parameters of the water column and watershed land cover on C emission pattern in the river waters. The PCA identified two factors that had generally low ability to describe the variance (19 and 7%, respectively; **Table S3** of the Supplement). None of the factors acted significantly on dissolved $CO_2$, $CH_4$ or $CO_2$ flux in the river water. The RDA treatment did not provide additional insights into environmental control of C pattern across the rivers and seasons. After normalization, the main result was that the analyses are not statistically significant ($p > 0.05$).

*3.4. Areal C emissions and export fluxes*

The C emissions (> 99.5 % $CO_2$, < 0.5 % $CH_4$) from the lotic waters of the Ket River basin were assessed based on total river water coverage of the Ket watershed in 2019 (856 km², of which 691 km² is seasonal water, according to the Global SDG database). Given that the measurements were performed at the peak of spring flood in 2019, we used the maximal water coverage of the Ket River basin to calculate the emissions during May and June, and baseflow coverage for measurements during July-October period.

For C emission calculation, we used the mean values of $FCO_2$ of the main stem and the tributaries ($1.31 \pm 0.81$ g C $m^{-2}$ $d^{-1}$ for spring flood; $2.11 \pm 1.86$ g C $m^{-2}$ $d^{-1}$ for summer-autumn baseflow) which covers full variability of both tributaries and the Ket River main channel (**Table 1, Figure 3**). For the month of July

which was not sampled in this work and which represents a transition period between the flood and the baseflow, we used the mean value of May and August (1.55 g C $m^{-2}$ $d^{-1}$). For the two months of maximal water flow (May - June), the C emission from the whole Ket basin amounts to 68±42 Gg. When summed up with July (25±20 Gg) and summer-autumn baseflow period (August to October) emission (32±28 Gg), the total open water season emission flux is 125 Gg. The uncertainty on the total emission over 6 months of the open water period is difficult to quantify but it can be estimated as between 30 and 50 %. This range covers both the uncertainty of the water coverage of the territory (i.e., Krickov et al., 2021) and the seasonal and spatial variations of $CO_2$ emission in the Ket basin assessed in the present study.

Based on yield calculations described in section 2.4, the total annual (excluding ice-covered period) riverine C export from the Ket River basin ($S_{watershed}$ = 94,000 km²) is 0.35 Tg (3.7 t C $km^{-2}_{land}$ $y^{-1}$), of which DOC, DIC and POC accounts for 56, 24 and 20%, respectively. Therefore, over the 6 month of open water period, the C emissions from lotic waters of Ket watershed constituted less than 30% of the dissolved and particulate downstream export of carbon.

## 4. DISCUSSION

### *4.1. Temporal and spatial pattern of $CO_2$ emissions from the river waters*

The first important result of the present study is quite low spatial and seasonal variability in both $CO_2$ concentration and emissions, as well as in DOC concentration and aromaticity (reflected by $SUVA_{254}$) in the main channel (**Fig. 3, S3, Table 1**). The variability in the tributaries was much larger, with differences in dissolved and gaseous C parameters between spring flood and summer-autumn baseflow (**Table S4 A**). While $CO_2$ concentrations were different between tributaries and the main stem during both flood and baseflow, the $CO_2$ flux was not different between the main stem and tributaries regardless of season (**Table S4 B**). This, together with lack of diel variations in $CO_2$ concentrations and emissions during spring period of maximal water coverage (**Fig. 4**), suggest rather stable pattern of $CO_2$ in the river water, not linked to short-scale processes (primary productivity, photolysis, daily temperature variation). Indeed, negligible primary productivity in the water column may stem from low water temperatures (9.3 °C), shallow photic layer of

organic-rich waters (DOC of 22 mg $L^{-1}$) and lack of periphyton activity during high flow of the spring flood. Note that this finding contrasts the recent results of high frequency $pCO_2$ measurements in temperate rivers that show a 30 % higher nocturnal emission compared to daytime observations due to photosynthesis/respiration cycle (Gómez-Gener et al., 2021b). In the Ambolikha River of Eastern Siberia, a small ($S_{watershed}$ = 121 km²) Arctic stream of continuous permafrost zone, the diel $CO_2$ cycle exhibited a moderate increase during the day, which was attributed to external lateral sources and photochemical oxidation of terrestrial DOC, rather than in-stream metabolism (Castro-Morales et al., 2022). At the same time, several studies in tropical DOM-rich rivers such as Congo (Borges et al. 2019) have not detected diel variations of $CO_2$ because aquatic pelagic primary production was low (Descy et al., 2018) due to strong light attenuation in the water column by DOM.

Concerning spatial variability of C concentrations and emissions during the spring flood, the $pCO_2$ did not demonstrate sizable variation along the main stem of the Ket River and some of its tributaries, when moving from the mouth to the headwaters. The SUVA also remained highly stable along the river flow. This, together with a lack of $FCO_2$ correlation with river watershed area during this period (**Table 2**) and the absence of link between the stream's Strahler order and measured $FCO_2$ and $K_T$ (**Fig. S5 B, C**), suggest relatively modest control of headwater C cycling by 'fresh' unprocessed organic matter from upland mire waters on $CO_2$ emissions from the Ket River basin. Much stronger control of mire waters is reported in boreal zone of the Northern Europe (Wallin et al., 2013, 2018). Furthermore, our results on the Ket River main stem and tributaries are in contrast to the general view of disproportional importance of headwater streams in overall $CO_2$ emission from river basins (Li et al., 2021). Thus, across the United States fluvial system, the stream's Strahler order was shown to be important driver of $CO_2$ evasion from river water surfaces, with lower order streams exhibiting the highest $pCO_2$ and gas transfer velocity (Butman and Raymond, 2011). A likely explanation is relative low values of gas transfer velocity measured in the small streams of the Ket basin in this study (0.2 - 2.0 m $d^{-1}$, **Table 1**). Based on a hydraulic model of stream velocity and mean channel slope (Eqn. 4 in Raymond et al., 2012), we calculated the gas transfer velocities in studied rivers as median of 1.02, IQR from 0.27 to 1.52 m $d^{-1}$, in very good agreement with chamber-measured values for the Ket River main stem and tributaries. Although these calculated values are also consistent with transfer coefficients

for western Siberia calculated by Liu et al. (2022) based on reach-slope and flow velocity (i.e., $K_T \leq 2$ m $d^{-1}$), they are typical of lakes rather than rivers (i.e., Kokic et al., 2015). We believe that low $K_T$ values for the Ket River basin stem from low channel slope (0.2 to 0.7 m $km^{-1}$) and flow rate (1-2 km $h^{-1}$), strongly forested and wind-protected river bed without distinct valley due to generally flat orographic context of this part of the WSL (Serikova et al., 2018). Furthermore, due to small size and short fetch of the Ket River and its tributaries (see pictures of typical environments in **Fig. S4 B-D** of the Supplement), extended floodplain zone also contributes to low values of $K_T$ measured in the studied river basin. This is consistent with observations in other flooded regions, where a canopy of vegetation protects the water-air interface from wind stress thus rendering the gas transfer velocity lower compared to open water such as large river (i.e., Foster-Martinez and Variano, 2016; Ho et al., 2018; Abril and Borges, 2019). We therefore warn against the use of high value of transfer velocity, suitable for large Siberian rivers (i.e., Karlsson et al., 2021; Vorobyev et al., 2021), for assessing the emissions in medium and small size, sheltered streams with extensive riparian vegetation. Another important aspect linked to C emissions from flooded forest (notably birch trees, see **Fig. S4 B**) of the floodplain (e.g. Pangala et al., 2017), not investigated in this study.

*4.2. Environmental factors possibly controlling $CO_2$ concentration and emission pattern in the Ket River main stem and tributaries*

Despite sizable variability of $pCO_2$ in the tributaries, especially during the baseflow, there were no correlations between either $pCO_2$ or $FCO_2$ and main hydrochemical parameters of the water column (**Table 2**). The only exception is $O_2$ concentration, which negatively correlated with $pCO_2$ during spring flood and both $pCO_2$ and $FCO_2$ during summer baseflow (**Fig. 5 A**). This finding suggests potential importance of shallow suboxic riparian flooded zone, meadows and forest, as well as floodplain lakes, in controlling $CO_2$ build up in the water column due to diffusion from sediments or decaying macrophytes, as it was shown for the floodplain of the Ob River middle course (Krickov et al., 2021). We believe that main reasons of remarkable stability in $CO_2$ concentrations and emissions and weak environmental control on dissolved and gaseous pattern in the Ket River basin are (1) essentially homogeneous landscapes, lithology and quaternary deposits of the whole river basin (20-25 % bogs, 60-70% forest, 3-5 % riparian zone), and (2) strong

dominance of allochthonous sources in both dissolved and particulate organic matter. Indeed, the SUVA and bacterial number (TBC) positively correlated with both $pCO_2$ and $FCO_2$ during summer (**Fig. 5 B; Table 2**), which may indicate non-negligible role of bacterial processing of allochthonous (aromatic) DOC delivered to the water column from wetlands and mires. As such, homogeneous land cover and essentially allochthonous DOC can still lead to variations of $CO_2$ per stream size, with small systems showing higher values than large systems as predicted conceptually (Hotchkiss et al., 2015) and verified at basin-scale (e.g. Borges et al., 2019). Consistent with this, we observed systematically higher $CO_2$ concentration and flux in small tributaries [which were fed by mire waters with 'non-processed' OM] compared to the main stem (**Table 2**). Furthermore, the positive correlation between mean annual precipitation (MAP) and $pCO_2$ and $FCO_2$ during the baseflow (**Table 2, Fig. 5 D**) could reflect the importance of water storage in the mires and wetlands (which also showed positive but less significant correlations, **Table 2**) during the summer time, and progressive release of $CO_2$ and DOC-rich waters from the wetlands to the streams. Another indirect evidence of the mire water control on $CO_2$ emission from the river cmes from daily $CO_2$ pattern in a tributary of the Ket River (**Fig. 4 E**). For this relatively small river ($S_{watershed}$ = 472 km²), we noted that there was quite heavy rainfall, between 7 am and 3 pm, prior to the $CO_2$ peak which was observed at 7 pm. Given that water residence time is very short during spring flood, when the soils are partially frozen, the delivery of allochtonous DOM and elevated $CO_2$ from adjacent mires could be the cause of observed $CO_2$ peak. Generally, the terrestrial source controlling $CO_2$ pattern in the Ket River could be either soil litter leachates (in spring) or bog water (during baseflow, when the river water is substantially derived from wetlands, Ala-aho et al., 2018a, b). Therefore, the patterns in $CO_2$ emissions observed in the present study during summer baseflow thus suggest the importance of allochthonous organic matter from the peatland for $CO_2$ production in the water column and in soils where the degradation of DOC is enhanced by the presence of bacteria. This is consistent with observations in other regions that, during summer-time, numerous processes contribute to increase $CO_2$ in rivers such as higher temperature stimulating microbial metabolism, longer residence time and enhanced flow paths of soil water (Borges et al. 2018).

A correlation between $CO_2$ flux during baseflow and the proportion of deciduous needleleaf forest at the watershed (**Fig. 5 C**) may suggest the importance of C cycling by larch trees and their possible control on

491 the delivery of degradable organic matter to the river. Similar control of larch vegetation on riverine $CO_2$ has
492 been suggested for the Lena River, Eastern Siberia (Vorobyev et al., 2021) although we acknowledge that
493 further observations on contrasted Siberian watersheds are necessary to confirm the observation that larch
494 trees litterfall led to export of degradable OM to the river.

495 In the Ket River basin, the local soil/groundwater effects are expected to be more pronounced during
496 baseflow, due to lower impact of dilution, compared to the spring flood period. The hypothesis of deeper flow
497 path in summer compared to spring is confirmed for the WSL (Frey and McClelland, 2009; Pokrovsky et al.,
498 2015; Serikova et al., 2018) and is supported in this study by a strong increase in DIC concentration between
499 spring and summer (**Fig. 3**). Thus, although the pairwise correlations between parameters do not support any
500 particular mechanism, it is not excluded that OM bio- and photo degradation and local mire water feeding
501 drive $FCO_2$ in spring, and that deeper flowpaths and DIC export drive the elevated $FCO_2$ in summer. The
502 latter is consistent with results of analysis of streams and rivers across the contiguous United States, which
503 demonstrated that ~60% of $CO_2$ evasion is from external sources rather than internal production (Hotchkiss
504 et al., 2015). In view of lack of correlation of $CO_2$ emissions in the Ket River and tributaries with
505 hydrochemical parameters of the water column, we believe that external source of $CO_2$ in studied river system
506 represents sizable contribution to total riverine $CO_2$ evasion across the seasons and sampling sites. In
507 particular, in small peatland streams, the $CO_2$-rich deep peat/groundwater is known to be the major source of
508 aquatic $CO_2$ under low flow conditions (Dinsmore and Billett, 2008), whereas in boreal headwater streams
509 of N Sweden the main source of stream $CO_2$ was inflowing $CO_2$-rich soil waters (Winterdahl et al., 2016).

510 Another important factor responsible for higher $CO_2$ production in the water column in summer
511 compared to spring could be POC degradation. The riverine POC is known to be much more biodegradable
512 than DOC (Attermeyer et al., 2018), and the POC concentration in the Ket River basin increased 4-fold
513 between spring and summer (**Table 1**). The origin of summer-time POC and its lability remain elusive, but
514 could be a combination of plankton bloom and mire- or forest-derived DOC coagulation products in the water
515 column (Krickov et al., 2018). Furthermore, pronounced heterogeneity in $CO_2$ emission during baseflow
516 among tributaries may also reflect the heterogeneity of riverine organic matter which is known to be the
517 maximal during low flow conditions and minimal during high flow (Lynch et al., 2019).

The main unexpected result of this study is that none of the physiochemical parameters of the water column and the land cover factor is sufficiently strong to drive the $CO_2$ and $CH_4$ patterns, although they show pronounced spatial and seasonal variations. Although correlations do not necessary imply causation and some correlations could be spurious or indirect, this analysis, together with PCA treatment, allow first order assessment of possible governing factors or dismissing the environmental parameters that do not contribute in GHG pattern control. A likely explanation is that simultaneous operation of multiple aquatic processes that include carbon, oxygen, nutrient, and plankton and peryphyton dynamics as well as sediment respiration control the $CO_2$ and $CH_4$ exchanges with the atmosphere, as it is known for boreal lakes and floodplain zones of the boreal rivers (i.e., Bayer et al., 2019; Zabelina et al., 2021; Krickov et al., 2019). Given that even a multiparametric statistical treatment (PCA) did no demonstrate sizable explanation capacity of the data set, we cannot exclude that these potential physico-chemical, microbiological and landscape drivers are working in different (opposing) directions and have counteracted each other. However, further in-depth analysis of these interactions requires much better seasonal resolution, ideally over full period of the year, which was beyond the scope of the present study.

*4.3. Emissions from the Ket River basin compared to downstream export of riverine carbon*

The estimated C emissions (> 99.5 % C; < 0.5 % $CH_4$) from the Ket River main channel over 830 km distance (0.5 to 2.5 g C $m^{-2}$ $d^{-1}$) are comparable to those of the Ob River main channel (1.32±0.14 g C $m^{-2}$ $d^{-1}$ in the permafrost-free zone; Karlsson et al., 2021). The $CO_2$ emission in Ket's tributaries (1 to 2 g C $m^{-2}$ $d^{-1}$ in spring; 1 to 5 g C $m^{-2}$ $d^{-1}$ in summer) are within the range reported for small rivers and streams of the permafrost-free zone of western Siberia (0 to 3.6 g C $m^{-2}$ $d^{-1}$ in spring; 4 to 9 g C $m^{-2}$ $d^{-1}$ in summer; Serikova et al., 2018), forest and wetland headwater streams of northern Sweden (0.5 to 5 g C $m^{-2}$ $d^{-1}$; Gómez-Gener et al., 2021a), and boreal streams in Canada and Alaska (0.8 to 5.2 g C $m^{-2}$ $d^{-1}$, Koprivnjak et al., 2010; Teodoru et al., 2009; Crawford et al., 2013; Campeau et al., 2014). Total C emissions from the water surfaces of the Ket River basin assessed in this study (148 g C-$CO_2$ $m^{-2}_{water}$ $y^{-1}$, assuming no emission under ice), when normalized to the Ket river basin area ($S_{watershed}$ = 94,000 $km^2$), amounts to 1.35 g C $m^{-2}_{land}$ $y^{-1}$. Generally higher land area - specific emissions, comparable or exceeding those of the Ket River, were reported in

Québec (1.0 to 4.6 g C $m^{-2}$ $y^{-1}$; Campeau and del Giorgio, 2014; Hutchins et al., 2019; Teodoru et al., 2009), Sweden (1.6 to 8.6 g C $m^{-2}$ $y^{-1}$; Humborg et al., 2010; Jonsson et al., 2007; Lundin et al., 2013; Wallin et al., 2011, 2018) and boreal portions of the Yukon River (7 to 9 g C $m^{-2}$ $y^{-1}$; Striegl et al., 2012; Stackpoole et al., 2017). Possible reasons for these differences could be different areal coverage of the territory by river network, the calculated rather than measured $CO_2$ fluxes, or the higher gas transfer velocity in the rivers from mountainous regions.

The regional assessment of the Ket River basin performed in this study are based on direct chamber measurements of emissions and as such provide rigorous basis for upscaling the $CO_2$ emissions from currently understudied lotic waters of permafrost-free zone of Western Siberia. The C evasion from the fluvial network of the Ket River assessed in the present work (127 ± 11 Gg $y^{-1}$, ignoring the emission during the ice breakup in early spring) is 3 times lower than the total (DOC+DIC+POC) downstream export by this river from the same territory (0.35 Tg C $y^{-1}$ ). The riverine C yield for the Ket River (3.7 t C $km^{-2}_{land}$ $y^{-1}$) is in agreement with regional C (DOC+DIC) yield by permafrost-free small and medium size rivers of the WSL (3 to 4 t C $km^{-2}_{land}$ $y^{-1}$, Pokrovsky et al., 2020) and with the Ob River in the permafrost-free zone (3.6 t C $km^{-2}_{land}$ $y^{-1}$, Vorobyev et al., 2019). Note that the latter study of the Ob River, which is very similar in the environmental context to the Ket River, included high frequency weekly sampling over several years of monitoring. Thus, the similarity of downstream export fluxes of the Ket and Ob Rivers support the validity of approaches for sampling and C yield calculation employed in the present study. Such high C yields in the southern, permafrost-free part of the WSL stem from essentially inorganic carbon originated from groundwater discharge of carbonate mineral rich reservoirs, abundant in this region (Pokrovsky et al., 2015). At the same time, the organic C yield in rivers of this region is quite low and represents less than 20 % of total C yield (Pokrovsky et al., 2020; Vorobyev et al., 2019). This can explain anomalously low value of C evasion : C export of the Ket River (1 : 3) measured in this work as compared to the average values for permafrost-free zone of Western Siberia (1 : 1, Serikova et al., 2019). Another factor potentially leading to underestimation of C evasion in this study is GIS-based minimal water coverage which does not include seasonal oxbow lakes, flooded forest and temporary water bodies of the floodplain which provide sizable emissions (see Krickov et al., 2021). We also do not exclude that some important hot moments / hot spots of C emission were missed

in our sampling campaign, such as summer baseflow/autumn peaks (Serikova et al., 2019) or stagnant zones of the floodplain in summer (Krickov et al., 2021; Castro-Morales et al., 2021). This calls a need for higher spatial and temporal resolution monitoring of C emission, with special focus on important events across full hydrological continuum.

## 5. Concluding remarks

Via combination of discrete floating chamber and hydrochemistry and continuous $CO_2$ concentration measurements over 830 km of large pristine boreal river of western Siberia main channel and its 26 tributaries during the peak of spring flood and the summer-autumn baseflow, we quantified spatial and temporal variations, overall emissions of C ($CO_2$, $CH_4$) and export of (DOC, DIC and POC) during the 6 months of open water period. The range of $CO_2$ and $CH_4$ concentrations in the main channel and tributaries as well as $CO_2$ emissions were consistent with other boreal and subarctic regions but demonstrated rather low seasonal and spatial variability. The diel $CO_2$ flux by floating chambers and continuous $pCO_2$ measurements in the tributaries of the Ket River during spring flood demonstrated negligible impact of day/night period on the $CO_2$ concentrations and emission fluxes.

We hypothesize that homogeneous landscape coverage (bog and taiga forest) provide stable allochthonous input of DOM as confirmed by very weak spatial and seasonal variations of DOM aromaticity. Among possible driving factors of $CO_2$ production in the water column (bio- and photo-degradation of DOC and POC, plankton metabolism), none seems to be sizably important for persistent $CO_2$ supersaturation and relevant emissions. The landscape factors of the watershed (bog and forest coverage, soil organic carbon stock) of the tributaries and along the main stem did not sizably affected the C concentration and emission pattern across two seasons. We hypothesize that stable terrestrial input of strongly aromatic DOM, shallow photic layer and humic waters of the Ket River basin preclude sizable daily and seasonal variations of C parameters. Punctual discharge of groundwater, resuspension of sediments or shallow subsurface influx from mires and riparian zone may be responsible for small-scale heterogeneities in C emissions and concentrations along the main stem and among the tributaries. These effects are much stronger pronounced during summer

baseflow compared to spring flood. Overall, deeper flow paths in summer compared to spring enhance the DIC discharge within the river bed and the tributaries, thus leading to elevated $CO_2$ flux in summer. Additional factor responsible for higher $CO_2$ emission during this season could be mire-originated particulate organic matter (POM) processing in the water column.

The six month open-water period C emissions from the lotic waters of the Ket River basin were sizably lower than the downstream total C export by this river during the same period. We conclude that regional estimations of C balance in lotic systems should be based on a combination of direct chamber measurements, discrete hydrochemical sampling and continuous in-situ monitoring with submersible sensors, at least during two most important hydrological periods of the year which are, for boreal regions, the spring flood and the summer-autumn baseflow. We believe that this is the best trade-off between scientific rigor and logistical feasibility in poorly accessible, pristine and strongly understudied regions.

**Acknowledgements.**

We acknowledge support from RSF grant 22-17-00253, the TSU Development Program "Priority-2030", and the Swedish Research Council (grant no. 2016-05275).

**Authors contribution.**

AL and OP designed the study and wrote the paper; AL, SV, IK and OP performed sampling, analysis and their interpretation; LS performed bacterial assessment and DOC/DIC analysis and interpretation; MK performed landscape characterization of the Ket River basin and calculated water surface area; SK performed hydrological analysis; JK provided analyses of literature data, transfer coefficients for $FCO_2$ calculations and global estimations of areal emission vs export.

**Competing interests.**

The authors declare that they have no conflict of interest.

**Data availability.**

Pokrovsky, O., Lim, A., Krickov, I., Korets, M., Vorobyev, S.: "Ket River hydrochemistry, $CO_2$ concentration and landscape parameters", Mendeley Data, V1, doi: 10.17632/snwbkvg6tc.1, 2022.

**References**

Abril, G., Martinez, J.-M., Artigas, L. F., Moreira-Turcq, P., Benedetti, M. F., Vidal, L., Meziane, T., Kim, J.-H., Bernardes, M. C., Savoye, N., Deborde, J., Albéric, P., Souza, M. F. L., Souza, E. L., and Roland, F.: Amazon river carbon dioxide outgassing fueled by wetlands, Nature, 505, 395-398, https://doi.org/10.1038/nature12797, 2014.

Abril, G. and Borges, A. V.: Ideas and perspectives: Carbon leaks from flooded land: do we need to replumb the inland water active pipe? Biogeosciences, 16, 769–784, https://doi.org/10.5194/bg-16-769-2019, 2019.

Ala-Aho, P., Soulsby, C., Pokrovsky, O. S., Kirpotin, S. N., Karlsson, J., Serikova, S., Manasypov, R., Lim, A., Krickov, I., Kolesnichenko, L. G., Laudon, H., and Tetzlaff, D.: Permafrost and lakes control river isotope composition across a boreal Arctic transect in the Western Siberian lowlands, Environ. Res. Lett., 13, https://doi.org/10.1088/1748-9326/aaa4fe, 2018a.

Ala-aho, P., Soulsby, C., Pokrovsky, O. S., Kirpotin, S. N., Karlsson, J., Serikova, S., Vorobyev, S. N., Manasypov, R. M., Loiko, S., and Tetzlaff, D.: Using stable isotopes to assess surface water source dynamics and hydrological connectivity in a high-latitude wetland and permafrost influenced landscape, J. Hydrol., 556, 279–293, https://doi.org/10.1016/j.jhydrol.2017.11.024, 2018b.

Alin, S. R., Rasera, M. D. F. F. L., Salimon, C. I., Richey, J. E., Holtgrieve, G. W., Krusche, A. V., and Snidvongs, A.: Physical controls on carbon dioxide transfer velocity and flux in low-gradient river systems and implications for regional carbon budgets, J. Geophys. Res. Biogeosciences, 116, https://doi.org/10.1029/2010JG001398, 2011.

Allen, G. H. and Pavelsky, T. M.: Global extent of rivers and streams, Science, 361, 585–588, https://doi.org/10.1126/science.aat0636, 2018.

Almeida, R. M., Pacheco, F. S., Barros, N., Rosi, E., and Roland, F.: Extreme floods increase $CO_2$ outgassing from a large Amazonian rive, Limnol. Oceanogr., 62, 989–999, https://doi.org/10.1002/lno.10480, 2017.

Amaral, J. H. F., Borges, A. V., Melack, J. M., Sarmento, H., Barbosa, P. M., Kasper, D., Melo, M. L., de Fex Wolf., D., da Silva, J. S., and Forsberg, B. R.: Influence of plankton metabolism and mixing depth on $CO_2$ dynamics in an Amazon floodplain lake, Sci. Total. Env. 630, 1381-1393, https://doi.org/10.1016/j.scitotenv.2018.02.331, 2018.

Amaral, J. H. F., Melack, J. M., Barbosa, P. M., Borges, A. V., Kasper, D., Cortes, A. C., Zhou, W., MacIntyre, S., and Forsberg, B. R.: Inundation, hydrodynamics and vegetation influences carbon dioxide concentrations in Amazon floodplain lakes, Ecosystem, 25(4), 911–930, https://doi.org/10.1007/s10021-021-00692-y, 2022.

Attermeyer, K., Catalán, N., Einarsdottir, K., Freixa, A., Groeneveld, M., Hawkes, J. A., Bergquist, J., and Tranvik, L. J.: Organic carbon processing during transport through boreal inland waters: particles as important sites, J. Geophys. Res. Biogeosciences, 123, 2412–2428, https://doi.org/10.1029/2018JG004500, 2018.

Bartalev, S. A., Egorov, V. A., Ershov, D. V., Isaev, A. S., Lupyan, E. A., Plotnikov, D. E., and Uvarov, I. A.: Remote mapping of vegetation land cover of Russia based on data of MODIS spectroradmeter, Mod. Probl. Earth Remote Sens. Space, 8, 285–302, 2018.

Bastviken, D., Sundgren, I., Natchimuthu, S., Reyier, H., and Gålfalk, M.: Technical Note: Cost-efficient approaches to measure carbon dioxide ($CO_2$) fluxes and concentrations in terrestrial and aquatic environments using mini loggers, Biogeosciences, 12, 3849–3859, https://doi.org/10.5194/bg-12-3849-2015, 2015.

Bayer, T. K., Gustafsson, E., Brakebusch, M., and Beer, C.: Future carbon emission from boreal and permafrost lakes are sensitive to catchment organic carbon loads, J. Geophys. Res. Biogeosciences, 124, 1827-1848, https://doi.org/10.1029/2018JG004978, 2019.

Borges, A. V., Darchambeau, F., Lambert, T., Bouillon, S., Morana, C., Brouyère, S., Hakoun, V., Jurado, A., Tseng, H-C., Descy, J.-P., and Roland, F. A. E.: Effects of agricultural land use on fluvial carbon dioxide, methane and nitrous oxide concentrations in a large European river, the Meuse (Belgium), Sci. Total Environ., 610-611, 342-355, https://doi.org/10.1016/j.scitotenv.2017.08.047, 2018.

Borges, A. V., Darchambeau, F., Teodoru, C. R., Marwick, T. R., Tamooh, F., Geeraert, N., Omengo, F. O., Guérin, F., Lambert, T., Morana, C., Okuku, E., and Bouillon, S.: Globally significant greenhouse gas

emissions from African inland waters, Nature Geoscience, 8, 637-642, https://doi.org/10.1038/NGEO2486, 2015.
Bussmann, I.: Distribution of methane in the Lena Delta and Buor-Khaya Bay, Russia, Biogeosciences, 10, 4641–4652, https://doi.org/10.5194/bg-10-4641-2013, 2013.
Butman, D. and Raymond, P.: Significant efflux of carbon dioxide from streams and rivers in the United States, Nature Geoscience, 4, 839–842. https://doi.org/10.1038/ngeo1294, 2011.
Cai, W.-J. and Wang, Y.: The chemistry, fluxes, and sources of carbon dioxide in the estuarine waters of the Satilla and Altamaha Rivers, Georgia, Limnol. Oceanogr., 43, 657–668, https://doi.org/10.4319/lo.1998.43.4.0657, 1998.
Campeau, A. and del Giorgio, P. A.: Patterns in $CH_4$ and $CO_2$ concentrations across boreal rivers: Major drivers and implications for fluvial greenhouse emissions under climate change scenarios, Glob. Change Biol., 20, 1075–1088, https://doi.org/10.1111/gcb.12479, 2014.
Campeau, A., Lapierre, J.-F., Vachon, D., and del Giorgio, P. A.: Regional contribution of $CO_2$ and $CH_4$ fluxes from the fluvial network in a lowland boreal landscape of Québec, Glob. Biogeochem. Cycles, 28, 57–69, https://doi.org/10.1002/2013GB004685, 2014.
Castro-Morales, K., Canning, A., Körtzinger, A., Göckede, M., Küsel, K., Overholt, W. A., Wichard, T., Redlich, S., Arzberger, S., Kolle, O., and Zimov, N.: Effects of reversal of water flow in an Arctic floodplain river on fluvial emissions of $CO_2$ and $CH_4$, J. Geophys. Res. Biogeosciences, 127, e2021JG006485, https://doi.org/10.1029/2021JG006485, 2022.
Chadburn, S. E., Krinner, G., Porada, P., Bartsch, A., Beer, C., Belelli Marchesini, L., Boike, J., Ekici, A., Elberling, B., Friborg, T., Hugelius, G., Johansson, M., Kuhry, P., Kutzbach, L., Langer, M., Lund, M., Parmentier, F.-J. W., Peng, S., Van Huissteden, K., Wang, T., Westermann, S., Zhu, D., and Burke, E. J.: Carbon stocks and fluxes in the high latitudes: using site-level data to evaluate Earth system models, Biogeosciences, 14, 5143–5169, https://doi.org/10.5194/bg-14-5143-2017, 2017.
Cooper, L. W., McClelland, J. W., Holmes, R. M., Raymond, P. A., Gibson, J. J., Guay, C. K., and Peterson, B. J.: Flow-weighted values of runoff tracers ($\delta^{18}O$, DOC, Ba, alkalinity) from the six largest Arctic rivers, Geophys. Res. Lett., 35, L18606, https://doi.org/10.1029/2008GL035007, 2008.
Crawford, J. T., Striegl, R. G., Wickland, K. P., Dornblaser, M. M., and Stanley, E. H.: Emissions of carbon dioxide and methane from a headwater stream network of interior Alaska, J. Geophys. Res. Biogeosciences, 118, 482–494, https://doi.org/10.1002/jgrg.20034, 2013.
Crawford, J. T., Loken, L. C., Casson, N. J., Smith, C., Stone, A. G., and Winslow, L. A.: High-speed limnology: using advanced sensors to investigate spatial variability in biogeochemistry and hydrology, Environ. Sci. Technol., 49, 442–450, https://doi.org/10.1021/es504773x, 2015.
Crawford, J. T., Stanley, E. H., Dornblaser, M. M., and Striegl, R. G.: $CO_2$ time series patterns in contrasting headwater streams of North America, Aquatic Sciences, 79, 473-486, https://doi.org/10.1007/s00027-016-0511-2, 2016a.
Crawford, J. T., Loken, L. C., Stanley, E. H., Stets, E. G., Dornblaser, M. M., and Striegl, R. G.: Basin scale controls on $CO_2$ and $CH_4$ emissions from the Upper Mississippi River, Geophys. Res. Lett., 43, 1973–1979, https://doi.org/10.1002/2015GL067599, 2016b.
Crawford, J. T., Butman, D. E., Loken, L. C., Stadler, P., Kuhn, C., and Striegl, R. G.: Spatial variability of $CO_2$ concentrations and biogeochemistry in the Lower Columbia River, Inland Waters, 7, 417-427, https://doi.org/10.1080/20442041.2017.1366487, 2017.
Dawson, J. J., Billett, M. F., Hope, D., Palmer, S. M., and Deacon, C.: Sources and sinks of aquatic carbon in a peatland stream continuum, Biogeochemistry, 70, 71–92, 2004.
Descy, J. P., Darchambeau, F., Lambert, T., Stoyneva, M. P., Bouillon, S., and Borges, A. V.: Phytoplankton dynamics in the Congo River, Freshwater Biology, 62, 87–101, https://doi.org/10.1111/fwb.12851, 2017.
DelDuco, E. M. and Xu, Y. J.: Dissolved carbon transport and processing in North America's largest swamp river entering the Northern Gulf of Mexico, Water, 11, 1395, https://doi.org/10.3390/w11071395, 2019.
Denfeld, B. A., Frey, K. E., Sobczak, W. V., Mann, P. J., and Holmes, R. M.: Summer $CO_2$ evasion from streams and rivers in the Kolyma River basin, north-east Siberia, Polar Res., 32, 19704, https://doi.org/10.3402/polar.v32i0.19704, 2013.

Dinsmore, K. J. and Billett, M. F.: Continuous measurement and modeling of $CO_2$ losses from a peatland stream during stormflow events, Water Resour. Res., 44, W12417, https://doi.org/10.1029/2008WR007284, 2008.

Dinsmore, K. J., Billett, M. F., and Dyson, K. E.: Temperature and precipitation drive temporal variability in aquatic carbon and GHG concentrations and fluxes in a peatland catchment, Glob. Change Biol., 19, 2133–2148, https://doi.org/10.1111/gcb.12209, 2013.

Feng, X., Vonk, J. E., Dongen, B. E. V., Gustafsson, Ö., Semiletov, I. P., Dudarev, O. V., Wang, Z., Montluçon, D. B., Wacker, L., and Eglinton, T. I.: Differential mobilization of terrestrial carbon pools in Eurasian Arctic river basins, Proc. Natl. Acad. Sci. U. S. A., 110, 14168–14173, https://doi.org/10.1073/pnas.1307031110, 2013.

Foster-Martinez, M. R. and Variano, E. A.: Air-water gas exchange by waving vegetation stems, J. Geophys. Res. Biogeosciences, 121, 1916–1923, https://doi.org/10.1002/2016JG003366, 2016.

Frey, K. E. and Smith, L. C.: How well do we know northern land cover? Comparison of four global vegetation and wetland products with a new ground-truth database for West Siberia. Glob. Biogeochem. Cycles, 21, GB1016. https://doi.org/10.1029/2006GB002706, 2007.

Frey, K. E. and McClelland, J. W.: Impacts of permafrost degradation on arctic river biogeochemistry, Hydrol. Process., 23, 169–182, https://doi.org/10.1002/hyp.7196, 2009.

Gómez-Gener, L., Rocher-Ros, G., Battin, T., Cohen, M. J., Dalmagro, H. J., Dinsmore, K. J., Drake, T. W., Duvert, C., Enrich-Prast, A., Horgby, Å., Johnson, M. S., Kirk, L., Machado-Silva, F., Marzolf, N. S., McDowell, M. J., McDowell, W. H., Miettinen, H., Ojala, A. K., Peter, H., Pumpanen, J., Ran, L., Riveros-Iregui, D. A., Santos, I. R., Six, J., Stanley, E. H., Wallin, M. B., White, S. A., and Sponseller, R. A.: Global carbon dioxide efflux from rivers enhanced by high nocturnal emissions, Nat. Geosci., 1–6, https://doi.org/10.1038/s41561-021-00722-3, 2021a.

Gómez-Gener, L., Hotchkiss, E. R., Laudon, H., and Sponseller, R. A.: Integrating discharge-concentration dynamics across carbon forms in a boreal landscape, Water Resour. Res., 57, e2020WR028806, https://doi.org/10.1029/2020WR028806, 2021b.

Griffin, C. G., McClelland, J. W., Frey, K. E., Fiske, G., and Holmes, R. M.: Quantifying CDOM and DOC in major Arctic rivers during ice-free conditions using Landsat TM and ETM+ data, Remote Sens. Environ., 209, 395–409, https://doi.org/10.1016/j.rse.2018.02.060, 2018.

Harris, I., Jones, P. d., Osborn, T. j., and Lister, D. h.: Updated high-resolution grids of monthly climatic observations – the CRU TS3.10 Dataset, Int. J. Climatol., 34, 623–642, https://doi.org/10.1002/joc.3711, 2014.

Ho, D. T., Engel, V. C., Ferrón, S., Hickman, B., Choi, J., and Harvey, J. W.: On factors influencing air-water gas exchange in emergent wetlands, J. Geophys. Res. Biogeosciences, 123, 178–192, https://doi.org/10.1002/2017JG004299, 2018.

Holmes, R. M., McClelland, J. W., Peterson, B.J ., & Tank S. E. et al. Seasonal and annual fluxes of nutrients and organic matter from large rivers to the Arctic Ocean and surrounding seas, Estuaries and Coasts, 35, 369-382. doi: 10.1007/s12237-011-9386-6, 2012.

Holmes, R. M., Coe, M. T., Fiske, G. J., Gurtovaya, T., McClelland, J. W., Shiklomanov, A. I., Spencer, R. G. M., Tank, S. E., and Zhulidov, A. V.: Climate change impacts on the hydrology and biogeochemistry of Arctic Rivers, in: Climatic Changes and Global warming of Inland Waters: Impacts and Mitigation for Ecosystems and Societies, edited by: Goldman, C. R., Kumagi, M., and Robarts, R. D., John Wiley and Sons, 1–26, 2013.

Hotchkiss, E. R., Hall Jr, R. O., Sponseller, R. A., Butman, D., Klaminder, J., Laudon, H., Rosvall, M., and Karlsson, J.: Sources of and processes controlling $CO_2$ emissions change with the size of streams and rivers, Nat. Geosci., 8, 696–699, https://doi.org/10.1038/ngeo2507, 2015.

Hugelius, G., Tarnocai, C., Broll, G., Canadell, J. G., Kuhry, P., and Swanson, D. K.: The northern circumpolar soil carbon database: Spatially distributed datasets of soil coverage and soil carbon storage in the northern permafrost regions, Earth Syst. Sci. Data, 5, 3–13, https://doi.org/10.5194/essd-5-3-2013, 2013.

Humborg, C., Mörth, C.-M., Sundbom, M., Borg, H., Blenckner, T., Giesler, R., and Ittekkot, V.: $CO_2$ supersaturation along the aquatic conduit in Swedish watersheds as constrained by terrestrial

786 respiration, aquatic respiration and weathering, Glob. Change Biol., 16, 1966–1978,
787 https://doi.org/10.1111/j.1365-2486.2009.02092.x, 2010.
788 Hutchins, R. H. S., Prairie, Y. T., and del Giorgio, P. A.: Large-Scale Landscape Drivers of $CO_2$, $CH_4$, DOC,
789 and DIC in Boreal River Networks, Glob. Biogeochem. Cycles, 33, 125–142,
790 https://doi.org/10.1029/2018GB006106, 2019.
791 Hutchins, R. H. S., Tank, S. E., Olefeldt, D., Quinton, W. L., Spence, C., Dion, N., Estop-Aragonés, C., and
792 Mengistu, S. G.: Fluvial $CO_2$ and $CH_4$ patterns across wildfire-disturbed ecozones of subarctic Canada:
793 Current status and implications for future change, Glob. Change Biol., 26, 2304–2319,
794 https://doi.org/10.1111/gcb.14960, 2020.
795 Johnson, M. S., Billett, M. F., Dinsmore, K. J., Wallin, M., Dyson, K. E., and Jassal, R. S.: Direct and
796 continuous measurement of dissolved carbon dioxide in freshwater aquatic systems—method and
797 applications, Ecohydrology, 3, 68–78, https://doi.org/10.1002/eco.95, 2009.
798 Jonsson, A., Algesten, G., Bergström, A.-K., Bishop, K., Sobek, S., Tranvik, L. J., and Jansson, M.:
799 Integrating aquatic carbon fluxes in a boreal catchment carbon budget, J. Hydrol., 334, 141–150,
800 https://doi.org/10.1016/j.jhydrol.2006.10.003, 2007.
801 Karlsson, J., Serikova, S., Vorobyev, S. N., Rocher-Ros, G., Denfeld, B., and Pokrovsky, O. S.: Carbon
802 emission from Western Siberian inland waters, Nat. Commun., 12, 825, https://doi.org/10.1038/s41467-
803 021-21054-1, 2021.
804 Kokic, J., Wallin, M. B., Chmiel, H. E., Denfeld, B. A., and Sobek, S.: Carbon dioxide evasion from
805 headwater systems strongly contributes to the total export of carbon from a small boreal lake catchment,
806 J. Geophys. Res. Biogeosciences, 120, 13–28, https://doi.org/10.1002/2014JG002706, 2015.
807 Koprivnjak, J.-F., Dillon, P. J., and Molot, L. A.: Importance of $CO_2$ evasion from small boreal streams, Glob.
808 Biogeochem. Cycles, 24, GB4003, https://doi.org/10.1029/2009GB003723, 2010.
809 Krickov, I. V., Lim, A. G., Manasypov, R. M., Loiko, S. V., Shirokova, L. S., Kirpotin, S. N., Karlsson, J.,
810 and Pokrovsky, O. S.: Riverine particulate C and N generated at the permafrost thaw front: Case study
811 of western Siberian rivers across a 1700 km latitudinal transect, Biogeosciences, 6867–6884,
812 https://doi.org/10.5194/bg-15-6867-2018, 2018.
813 Krickov, I. V., Serikova, S., Pokrovsky, O. S., Vorobyev, S. N., Lim, A. G., Siewert, M. B., and Karlsson, J.:
814 Sizable carbon emission from the floodplain of Ob River, Ecol. Indic., 131, 108164,
815 https://doi.org/10.1016/j.ecolind.2021.108164, 2021.
816 Lauerwald, R., Laruelle, G. G., Hartmann, J., Ciais, P., and Regnier, P. A. G.: Spatial patterns in CO2 evasion
817 from the global river network, Glob. Biogeochem. Cycles, 29, 534–554,
818 https://doi.org/10.1002/2014GB004941, 2015.
819 Leith, F. I., Dinsmore, K. J., Wallin, M. B., Billett, M. F., Heal, K. V., Laudon, H., Öquist, M. G., and Bishop,
820 K.: Carbon dioxide transport across the hillslope–riparian–stream continuum in a boreal headwater
821 catchment, Biogeosciences, 12, 1881–1892, https://doi.org/10.5194/bg-12-1881-2015, 2015.
822 Leng, P., Li, Z., Zhang, Q., Li, F., and Koschorreck, M.: Fluvial $CO_2$ and $CH_4$ in a lowland agriculturally
823 impacted river network: Importance of local and longitudinal controls, Environ. Pollution 303, Art No
824 119125, https://doi.org/10.1016/j.envpol.2022.119125, 2022.
825 Li, M., Peng, C., Zhang, K., Xu, L., Wang, J., Yang, Y., Li, P., Liu, Z., and He, N.: Headwater stream
826 ecosystem: an important source of greenhouse gases to the atmosphere, Water Res., 190, 116738,
827 https://doi.org/10.1016/j.watres.2020.116738, 2021.
828 Liu S., Kuhn, C., Amatulli, G., Aho, K., Butman, D.E., Allen, G.H., Lin, P., Pan, M., Yamazaki, D.,
829 Brinkerhoff, C., Gleason, C., Xia, X., and Raymond, P.A.: The importance of hydrology in routing
830 terrestrialcarbon to the atmosphere via global streams and rivers, PNAS 119 No. 11, e2106322119;
831 https://doi.org/10.1073/pnas.2106322119, 2022.
832 Lobbes, J. M., Fitznar, H. P., and Kattner, G.: Biogeochemical characteristics of dissolved and particulate
833 organic matter in Russian rivers entering the Arctic Ocean, Geochim. Cosmochim. Acta, 64, 2973–
834 2983, https://doi.org/10.1016/S0016-7037(00)00409-9, 2000.
835 Lorke A., Bodmer, P., Noss, C., Alshboul, Z., Koschorreck, M., Somlai-Haase, C., Bastviken, D., Flury, S.,
836 McGinnis, D.F., Maeck, A., Müller, D., and Premke, K.: Technical note: drifting versus anchored
837 flux chambers for measuring greenhouse gas emissions from running waters, Biogeosciences, 12,
838 7013–7024, https://doi.org/10.5194/bg-12-7013-2015, 2015.

Lundin, E. J., Giesler, R., Persson, A., Thompson, M. S., and Karlsson, J.: Integrating carbon emissions from lakes and streams in a subarctic catchment, J. Geophys. Res. Biogeosciences, 118, 1200–1207, https://doi.org/10.1002/jgrg.20092, 2013.

Lynch, L. M., Sutfin, N. A., Fegel, T. S., Boot, C. M., Covino, T. P., and Wallenstein, M. D.: River channel connectivity shifts metabolite composition and dissolved organic matter chemistry, Nat. Commun., 10, 459, https://doi.org/10.1038/s41467-019-08406-8, 2019.

Marie, D., Partensky, F., Vaulot, D., and Brussaard, C.: Enumeration of Phytoplankton, Bacteria, and Viruses in Marine Samples, Curr. Protoc. Cytom., 10, 11111–111115, https://doi.org/10.1002/0471142956.cy1111s10, 1999.

Pangala, S., Enrich-Prast, A., Basso, L., Peixoto, R. B., Bastviken, D., Hornibrook, E. R. C., Gatti, L. V., Ribeiro, H., et al.: Large emissions from floodplain trees close the Amazon methane budget, Nature 552, 230–234, https://doi.org/10.1038/nature24639, 2017.

Pekel, J.-F., Cottam, A., Gorelick, N., and Belward, A. S.: High-resolution mapping of global surface water and its long-term changes, Nature, 540, 418–422, https://doi.org/10.1038/nature20584, 2016.

Pokrovsky, O. S., Manasypov, R. M., Loiko, S., Shirokova, L. S., Krickov, I. A., Pokrovsky, B. G., Kolesnichenko, L. G., Kopysov, S. G., Zemtzov, V. A., Kulizhsky, S. P., Vorobyev, S. N., and Kirpotin, S. N.: Permafrost coverage, watershed area and season control of dissolved carbon and major elements in western Siberian rivers, Biogeosciences, 12, 6301–6320, https://doi.org/10.5194/bg-12-6301-2015, 2015.

Pokrovsky, O. S., Manasypov, R. M., Kopysov, S. G., Krickov, I. V., Shirokova, L. S., Loiko, S. V., Lim, A. G., Kolesnichenko, L. G., Vorobyev, S. N., and Kirpotin, S. N.: Impact of permafrost thaw and climate warming on riverine export fluxes of carbon, nutrients and metals in Western Siberia, Water (MDPI), 12, 1817, https://doi.org/10.3390/w12061817, 2020.

Pokrovsky, O. S., Manasypov, R. M., Chupakov, A. V., and Kopysov, S.: Element transport in the Taz River, western Siberia, Chemical Geology, 614, Art No 121180 https://doi.org/10.1016/j.chemgeo.2022.121180.2022.

Ran, L., Lu, X. X., Richey, J. E., Sun, H., Han, J., Yu, R., Liao, S., and Yi, Q.: Long-term spatial and temporal variation of $CO_2$ partial pressure in the Yellow River, China, Biogeosciences, 12, 921–932, https://doi.org/10.5194/bg-12-921-2015, 2015.

Ran, L., Lu, X. X., and Liu, S.: Dynamics of riverine $CO_2$ in the Yangtze River fluvial network and their implications for carbon evasion, Biogeosciences, 14, 2183–2198, https://doi.org/10.5194/bg-14-2183-2017, 2017.

Raymond, P. A., McClelland, J. W., Holmes, R. M., Zhulidov, A. V., Mull, K., Peterson, B. J., Striegl, R. G., Aiken, G. R., and Gurtovaya, T. Y.: Flux and age of dissolved organic carbon exported to the Arctic Ocean: A carbon isotopic study of the five largest arctic rivers, Glob. Biogeochem. Cycles, 21, GB4011, https://doi.org/10.1029/2007GB002934, 2007.

Raymond, P. A., Zappa, C.J., Butman, D., Bott, T.L., Potter, J., Mulholland, P., Laursen, A. E., McDowell, W. H., and Newbold, D.: Scaling the gas transfer velocity and hydraulic geometry in streams and small rivers. Limnology and Oceanography: Fluids and Environments, 2(1), 41-53. https://doi.org/10.1215/21573689-1597669, 2012.

Raymond, P. A., Hartmann, J., Lauerwald, R., Sobek, S., McDonald, C., Hoover, M., Butman, D., Striegl, R., Mayorga, E., Humborg, C., Kortelainen, P., Dürr, H., Meybeck, M., Ciais, P., and Guth, P.: Global carbon dioxide emissions from inland waters, Nature, 503, 355–359, https://doi.org/10.1038/nature12760, 2013.

Rehder, Z., Zaplavnova, A., and Kutzbach, L.: Identifying drivers behind spatial variability of methane concentrations in East Siberian ponds. Front. Earth Sci. 9, Art No 617662, doi: 10.3389/feart.2021.617662, 2021.

Rocher-Ros, G., Sponseller, R. A., Lidberg, W., Mörth, C.-M., and Giesler, R.: Landscape process domains drive patterns of $CO_2$ evasion from river networks, Limnol. Oceanogr. Lett., 4, 87–95, https://doi.org/10.1002/lol2.10108, 2019.

Santoro, M., Beer, C., Cartus, O., Schmullius, C., Shvidenko, A., McCallum, I., Wegmüller, U., and Wiesmann, A.: The BIOMASAR algorithm: An approach for retrieval of forest growing stock volume

using stacks of multi-temporal SAR data, in: Proceedings of ESA Living Planet Symposium, Bergen, Norway, 28 June – 2 July, 2010.
Schneider, C. L., Herrera, M., Raisle, M. L., Suarez, E., and Riveros-Iregui, D. A.: Carbon Dioxide ($CO_2$) Fluxes from terrestrial and aquatic environments in a high altitude tropical catchment. J Geophys. Res. Biogeosciences 125, e2020JG005844. https://doi.org/10.1029/2020JG005844, 2020.
Semiletov, I. P., Pipko, I. I., Shakhova, N. E., Dudarev, O. V., Pugach, S. P., Charkin, A. N., McRoy, C. P., Kosmach, D., and Gustafsson, Ö.: Carbon transport by the Lena River from its headwaters to the Arctic Ocean, with emphasis on fluvial input of terrestrial particulate organic carbon vs. carbon transport by coastal erosion, Biogeosciences, 8, 2407–2426, https://doi.org/10.5194/bg-8-2407-2011, 2011.
Serikova, S., Pokrovsky, O. S., Ala-Aho, P., Kazantsev, V., Kirpotin, S. N., Kopysov, S. G., Krickov, I. V., Laudon, H., Manasypov, R. M., Shirokova, L. S., Soulsby, C., Tetzlaff, D., and Karlsson, J.: High riverine $CO_2$ emissions at the permafrost boundary of Western Siberia, Nat. Geosci., 11, 825–829, https://doi.org/10.1038/s41561-018-0218-1, 2018.
Serikova, S., Pokrovsky, O. S., Laudon, H., Krickov, I. V., Lim, A. G., Manasypov, R. M., and Karlsson, J.: High carbon emissions from thermokarst lakes of Western Siberia, Nat. Commun., 10, https://doi.org/10.1038/s41467-019-09592-1, 2019.
Spawn, S. A., Dunn, S. T., Fiske, G. E., Natali, S. M., Schade, J. D., and Zimov, N. S.: Summer methane ebullition from a headwater catchment in Northeastern Siberia, Inland Waters, 5(3), 224-230, DOI: 10.5268/IW-5.3.845, 2015.
Stackpoole, S. M., Butman, D. E., Clow, D. W., Verdin, K. L., Gaglioti, B. V., Genet, H., and Striegl, R. G.: Inland waters and their role in the carbon cycle of Alaska, Ecol. Appl., 27, 1403–1420, https://doi.org/10.1002/eap.1552, 2017.
Stanley, E. H., Casson, N. J., Christel, S. T., Crawford, J. T., Loken, L. C., and Oliver, S.K.: The ecology of methane in streams and rivers: patterns, controls, and global significance, Ecol. Monogr. 86, 146–171, 2016.
Striegl, R. G., Dornblaser, M. M., McDonald, C. P., Rover, J. A., and Stets, E. G.: Carbon dioxide and methane emissions from the Yukon River system, Glob. Biogeochem. Cycles, 26, GB0E05, https://doi.org/10.1029/2012GB004306, 2012.
Teodoru, C. R., del Giorgio, P. A., Prairie, Y. T., and Camire, M.: Patterns in $pCO_2$ in boreal streams and rivers of northern Quebec, Canada, Glob. Biogeochem. Cycles, 23, GB2012, https://doi.org/10.1029/2008GB003404, 2009.
Tranvik, L., Cole, J. J., and Prairie, Y. T.: The study of carbon in inland waters-from isolated ecosystems to players in the global carbon cycle, Limnol. Oceanogr. Lett., 3, 41–48, https://doi.org/10.1002/lol2.10068, 2018.
Vachon, D., Sponseller, R. A., and Karlsson, J.: Integrating carbon emission, accumulation and transport in inland waters to understand their role in the global carbon cycle, Glob. Change Biol., 27, 719–727, https://doi.org/10.1111/gcb.15448, 2021.
Villa, J. A., Ju, Y., Yazbeck, T., Waldo, S., Wrighton, K. C., and Bohrer, G.: Ebullition dominates methane fluxes from the water surface across different ecohydrological patches in a temperate freshwater marsh at the end of the growing season, Sci. Total Environ. 767, 144498, 2021.
Vorobyev, S. N., Pokrovsky, O. S., Kolesnichenko, L. G., Manasypov, R. M., Shirokova, L. S., Karlsson, J., and Kirpotin, S. N.: Biogeochemistry of dissolved carbon, major, and trace elements during spring flood periods on the Ob River, Hydrol. Process., 33, 1579–1594, https://doi.org/10.1002/hyp.13424, 2019.
Vorobyev, S. N., Karlsson, J., Kolesnichenko, Y. Y., Korets, M. A., and Pokrovsky, O. S.: Fluvial carbon dioxide emission from the Lena River basin during the spring flood, Biogeosciences, 18, 4919–4936, https://doi.org/10.5194/bg-18-4919-2021, 2021.
Wallin, M. B., Öquist, M. G., Buffam, I., Billett, M. F., Nisell, J., and Bishop, K. H.: Spatiotemporal variability of the gas transfer coefficient ($KCO_2$) in boreal streams: Implications for large scale estimates of $CO_2$ evasion, Glob. Biogeochem. Cycles, 25, GB3025, https://doi.org/10.1029/2010GB003975, 2011.
Wallin, M. B., Grabs, T., Buffam, I., Laudon, H., Ågren, A., Öquist, M. G., and Bishop, K.: Evasion of $CO_2$ from streams – The dominant component of the carbon export through the aquatic conduit in a boreal landscape, Glob. Change Biol., 19, 785–797, https://doi.org/10.1111/gcb.12083, 2013.

Wallin, M. B., Campeau, A., Audet, J., Bastviken, D., Bishop, K., Kokic, J., Laudon, H., Lundin, E., Löfgren, S., Natchimuthu, S., Sobek, S., Teutschbein, C., Weyhenmeyer, G. A., and Grabs, T.: Carbon dioxide and methane emissions of Swedish low-order streams—a national estimate and lessons learnt from more than a decade of observations, Limnol. Oceanogr. Lett., 3, 156–167, https://doi.org/10.1002/lol2.10061, 2018.

Wild, B., Andersson, A., Bröder, L., Vonk, J., Hugelius, G., McClelland, J. W., Song, W., Raymond, P. A., and Gustafsson, Ö.: Rivers across the Siberian Arctic unearth the patterns of carbon release from thawing permafrost, PNAS, 116, 10280–10285, https://doi.org/10.1073/pnas.1811797116, 2019.

Winterdahl, M., Wallin, M. B., Karlsen, R. H., Laudon, H., Öquist, M., and Lyon, S. W.: Decoupling of carbon dioxide and dissolved organic carbon in boreal headwater streams, J. Geophys. Res. Biogeosciences, 121, 2630–2651, https://doi.org/10.1002/2016JG003420, 2016.

Yamamoto, S., Alcauskas, J. B., and Crozier, T. E.: Solubility of methane in distilled water and seawater. J. Chem. Eng. Data. 21, 78–80, 1976.

Zabelina, S. V., Shirokova, L. S., Klimov, S I., Chupakov, A. V., Lim, A. G., Polishchuk, Y. M., Polishchuk, V. M., Bogdanov, A. N., Muratov, I. N., Gueren, F., Karlsson, J., and Pokrovsky, O. S.: Seasonal and spatial variations of CO2 and CH4 concentrations and fluxes in surface waters of frozen peatlands (NE Europe): morphological and hydrochemical control, Limnology Oceanography, 66 (S1), S216-S230, doi: 10.1002/lno.11560, 2021.

Zolkos, S., Tank, S. E., Striegl, R. G., and Kokelj, S. V.: Thermokarst effects on carbon dioxide and methane fluxes in streams on the Peel Plateau (NWT, Canada), J. Geophys. Res. Biogeosciences, 124, 1781–1798, https://doi.org/10.1029/2019JG005038, 2019.

**Table 1.** Measured hydrochemical and GHG exchange parameters in the Ket River main stem and tributaries (average ± s.d.; (*n*) is number of measurements). The $FCO_2$ and $K_T$ are chamber-measured $CO_2$ flux and gas transfer velocity, respectively, whereas diffusive $CH_4$ flux ($FCH_4$) was calculated using chamber-specific transfer coefficient.

| | | Tributaries | | Main stem | |
|---|---|---|---|---|---|
| **Parameter** | **unit** | **Flood (*n*=26)** | **Base flow (*n*=12)** | **Flood (*n*=7)** | **Base flow (*n*=6)** |
| Water temperature | °C | 9.48±2.25 | 14.9±1.24 | 9.06±1.59 | 16.5±0.54 |
| pH | | 6.31±0.45 | 6.71±0.57 | 6.2±0.43 | 7.29±0.26 |
| Dissolved $O_2$ | mg $L^{-1}$ | 8.53±1.26 | 8.02±1.13 | 8.85±0.83 | 8.78±0.18 |
| Specific Conductivity | µS $cm^{-1}$ | 40.7±22.7 | 126.9±62.1 | 39±14.9 | 181±36.8 |
| DIC | mg $L^{-1}$ | 2.83±2.58 | 17.8±10.4 | 2.43±1.49 | 20.5±5.22 |
| DOC | mg $L^{-1}$ | 21.7±3.94 | 15.7±7.04 | 21.9±4.28 | 16.6±3.57 |
| $SUVA_{254}$ | L mg $C^{-1}$ $m^{-1}$ | 4.34±0.33 | 4.9±0.66 | 4.29±0.18 | 4.26±0.52 |
| PON | mg $L^{-1}$ | 0.08±0.06 | 0.64±0.27 | 0.1±0.07 | 0.96±0.22 |
| POC | mg $L^{-1}$ | 2.41±1.17 | 8±2.36 | 2.55±1.2 | 9.49±1.98 |
| TBC | $*10^5$ cells $ml^{-1}$ | 5.89±3.26 | 8.69±3.21 | 5.95±2.83 | 4.94±2.15 |
| $K_T$ | m $d^{-1}$ | 0.53±0.38 | 1.21±0.52 | 0.77±0.55 | 1.22±0.37 |
| $FCO_2$ | g C $m^{-2}$ $d^{-1}$ | 1.3±0.76 | 2.63±2.15 | 1.35±1.08 | 1.16±0.5 |
| $pCO_2$ | µatm | 2880±680 | 4000±1500 | 2400±330 | 2520±980 |
| $FCH_4$ | mmol C $m^{-2}$ $d^{-1}$ | 0.39±0.95 | 1.38±1.21 | 0.06±0.05 | 0.95±0.88 |
| $CH_4$ | µmol $L^{-1}$ | 0.65±0.66 | 1.17±0.81 | 0.17±0.01 | 0.86±0.91 |

**Table 2.** Pearson correlation coefficients of measured $FCO_2$, $CO_2$, and $CH_4$ concentration with hydrochemical parameters of the water column (DOC, SUVA, particulate organic carbon and nitrogen, total bacterial cells) and landscape parameters of the tributaries and the main stem of the Ket River. Significant ($p < 0.05$) values are labeled by asterisk.

| | all seasons | | | spring flood | | | summer baseflow | | |
|---|---|---|---|---|---|---|---|---|---|
| | $CH_4$ | $CO_2$ | $FCO_2$ | $CH_4$ | $CO_2$ | $FCO_2$ | $CH_4$ | $CO_2$ | $FCO_2$ |
| **Hydrochemical parameters** | | | | | | | | | |
| pH | 0.2 | -0.1 | -0.2 | -0.1 | 0.1 | -0.2 | 0.0 | -0.6* | -0.6* |
| Dissolved $O_2$ | -0.1 | -0.7* | -0.1 | 0.0 | -0.8* | 0.1 | -0.2 | -0.8* | -0.7* |
| Specific conductivity | 0.3 | 0.0 | 0.1 | -0.2 | 0.0 | 0.1 | 0.2 | -0.3 | -0.6* |
| DIC | 0.3 | 0.0 | 0.0 | -0.1 | 0.0 | 0.1 | 0.2 | -0.4 | -0.7* |
| DOC | -0.1 | 0.0 | 0.1 | 0.3 | 0.0 | -0.1 | -0.2 | -0.1 | 0.2 |
| $SUVA_{254}$ | 0.1 | 0.2 | 0.3 | 0.4 | -0.3 | 0.1 | -0.2 | 0.5* | 0.6* |
| PON | 0.1 | -0.1 | 0.2 | -0.2 | -0.4* | 0.2 | -0.4 | -0.5* | -0.5 |
| POC | 0.1 | -0.1 | 0.2 | -0.2 | -0.4* | 0.1 | -0.3 | -0.3 | 0.1 |
| TBC | 0.2 | 0.2 | 0.1 | 0.3 | -0.2 | -0.1 | 0.0 | 0.5* | 0.5* |
| **Climatic characteristics** | | | | | | | | | |
| MAAT | 0.2 | 0.0 | -0.5* | 0.1 | 0.0 | -0.4* | 0.2 | 0.1 | -0.5 |
| MAP | 0.0 | 0.3* | 0.5* | 0.1 | 0.0 | 0.3 | 0.1 | 0.6* | 0.7* |
| **Land-cover characteristics** | | | | | | | | | |
| Watershed area | -0.3 | -0.3* | 0.2 | -0.4 | -0.5* | 0.0 | -0.2 | -0.1 | 0.5 |
| Dark Needleleaf Forest | 0.1 | 0.0 | -0.3 | 0.1 | 0.0 | -0.3 | 0.2 | -0.1 | -0.2 |
| Light Needleleaf Forest | 0.3* | 0.4* | 0.2 | 0.4 | 0.2 | 0.0 | 0.4 | 0.7* | 0.6* |
| Broadleaf Forest | -0.3 | -0.4* | 0.1 | -0.5* | -0.4 | 0.1 | -0.3 | -0.6* | -0.2 |
| Mixed Forest | 0.0 | -0.2 | -0.3 | 0.1 | -0.1 | -0.3 | -0.1 | -0.4 | -0.4 |
| Peatlands and bogs | 0.0 | 0.2 | 0.3 | -0.1 | 0.0 | 0.2 | 0.1 | 0.2 | 0.4 |
| Riparian Vegetation | -0.1 | 0.0 | -0.1 | -0.2 | 0.1 | 0.0 | -0.2 | -0.2 | -0.5 |
| Grassland | 0.1 | -0.1 | 0.0 | -0.1 | -0.2 | 0.1 | 0.3 | 0.0 | -0.5 |
| Recent Burns | -0.1 | -0.1 | 0.2 | -0.1 | -0.2 | 0.1 | -0.3 | 0.1 | 0.4 |
| Water Bodies | -0.2 | -0.1 | 0.3 | -0.3 | -0.3 | 0.2 | -0.2 | -0.1 | 0.3 |

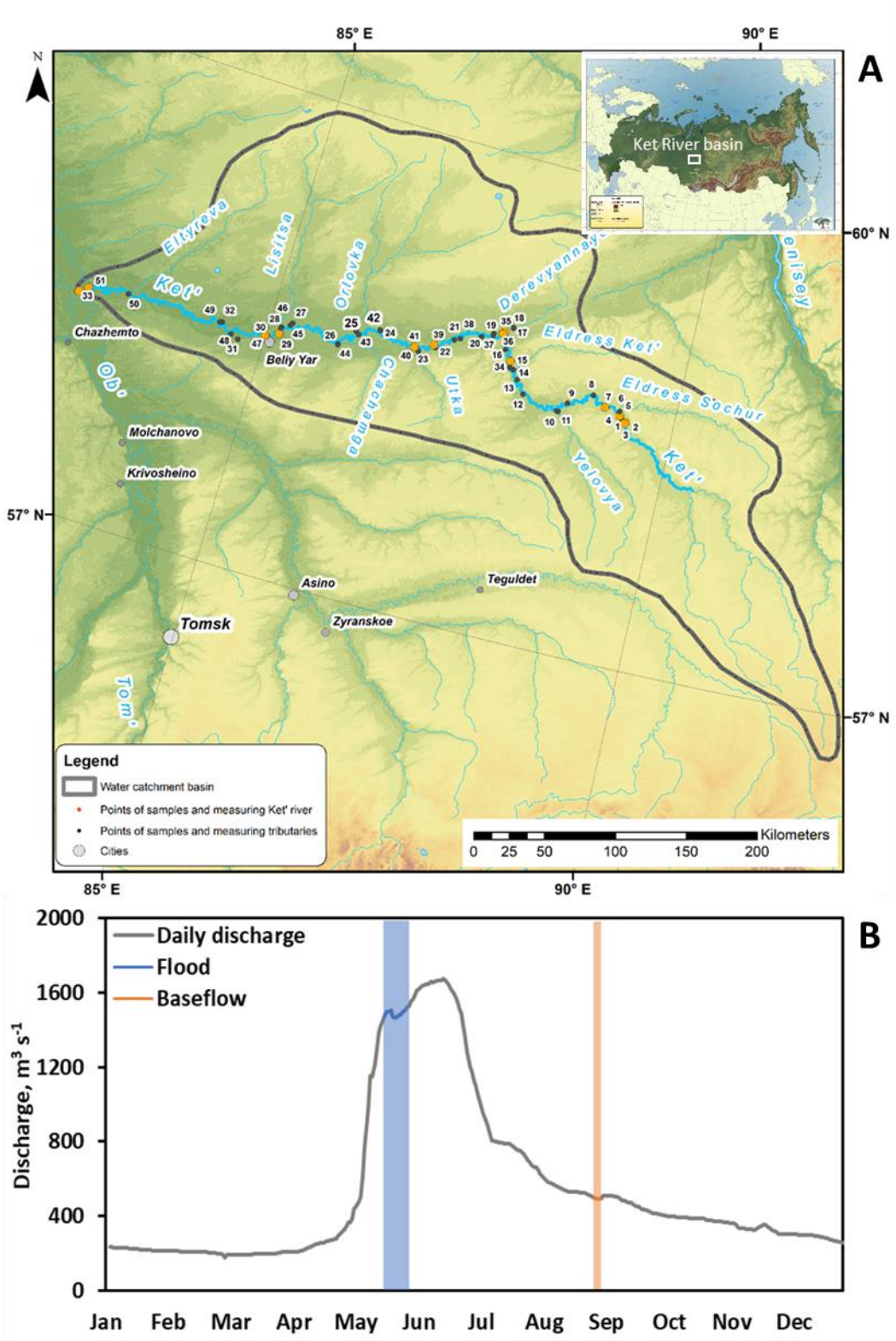


**Fig. 1. A:** Map of the studied Ket River watershed with continuous $pCO_2$ measurements in the main stem. **B:** Daily discharge (Q) at the gauging station of the Ket mouth, Rodionovka, in 2019. Highlighted in blue and orange are two sampling campaigns of this study, spring flood and summer-autumn baseflow.

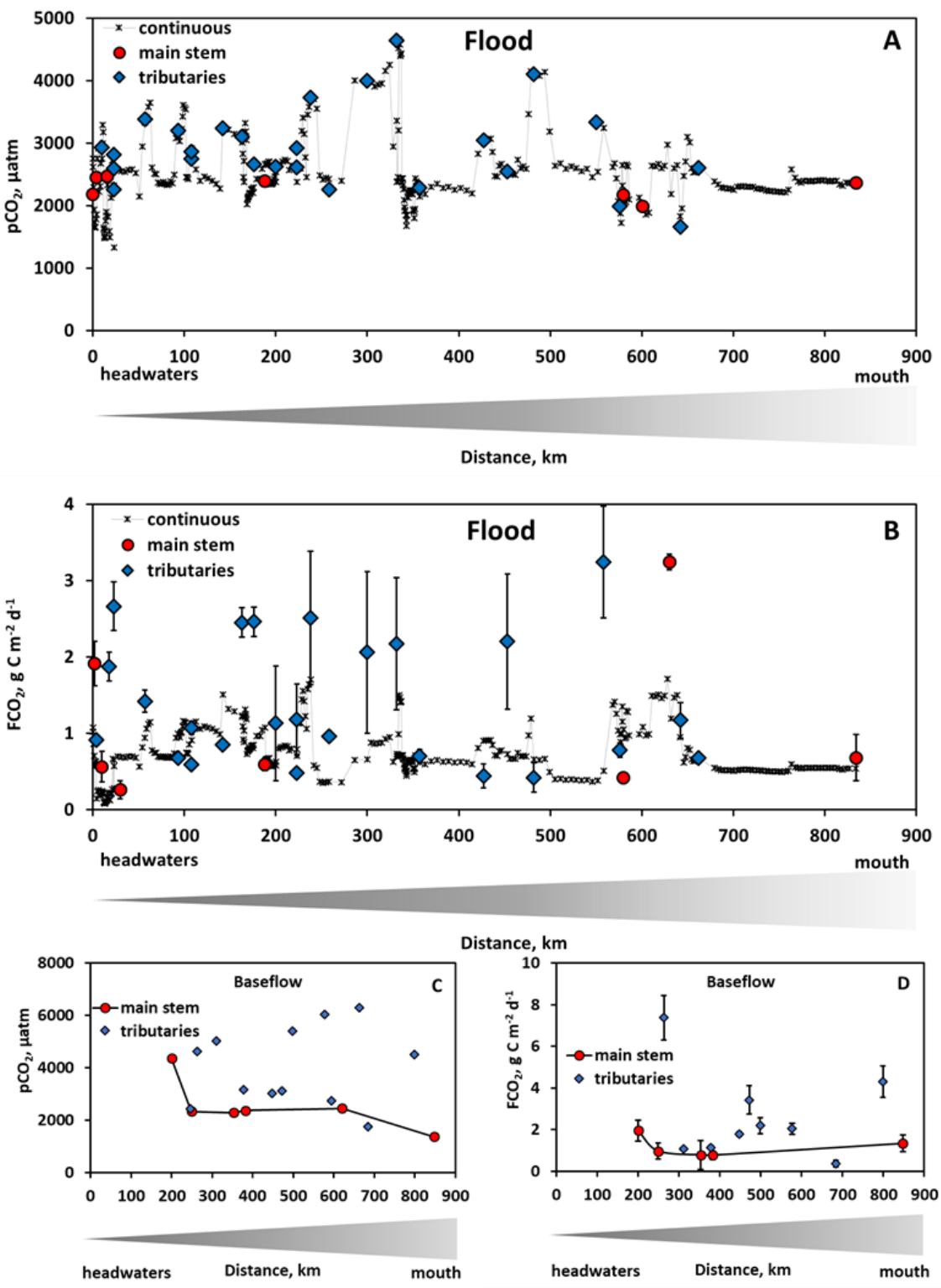


**Figure 2.** The measured $pCO_2$ (**A, C**) and $CO_2$ fluxes (**B, D**) during spring flood (**A, B**) and summer baseflow (**C, D**) of the Ket River main stem and tributaries (over the 830 km distance, from the headwaters to the mouth (left to right). The symbols represent discrete in situ $pCO_2$ (Vaissala) and $FCO_2$ (floating chambers) measurements of the main stem (red circles) and tributaries (blue diamonds). Continuous in-situ $pCO_2$ measurements and calculated $FCO_2$ are available only for the main stem in spring (black crosses). For the latter, we used an average value of measured gas transfer velocity ($K_T$) between two chamber sites (separated by a distance of 50 to 100 km) to calculate the $FCO_2$ from in-situ measured $pCO_2$ in the river section between these two sites. Note that during summer baseflow, the water level did not allow reaching the headwaters of the Ket River (first 0-200 km on the river course).

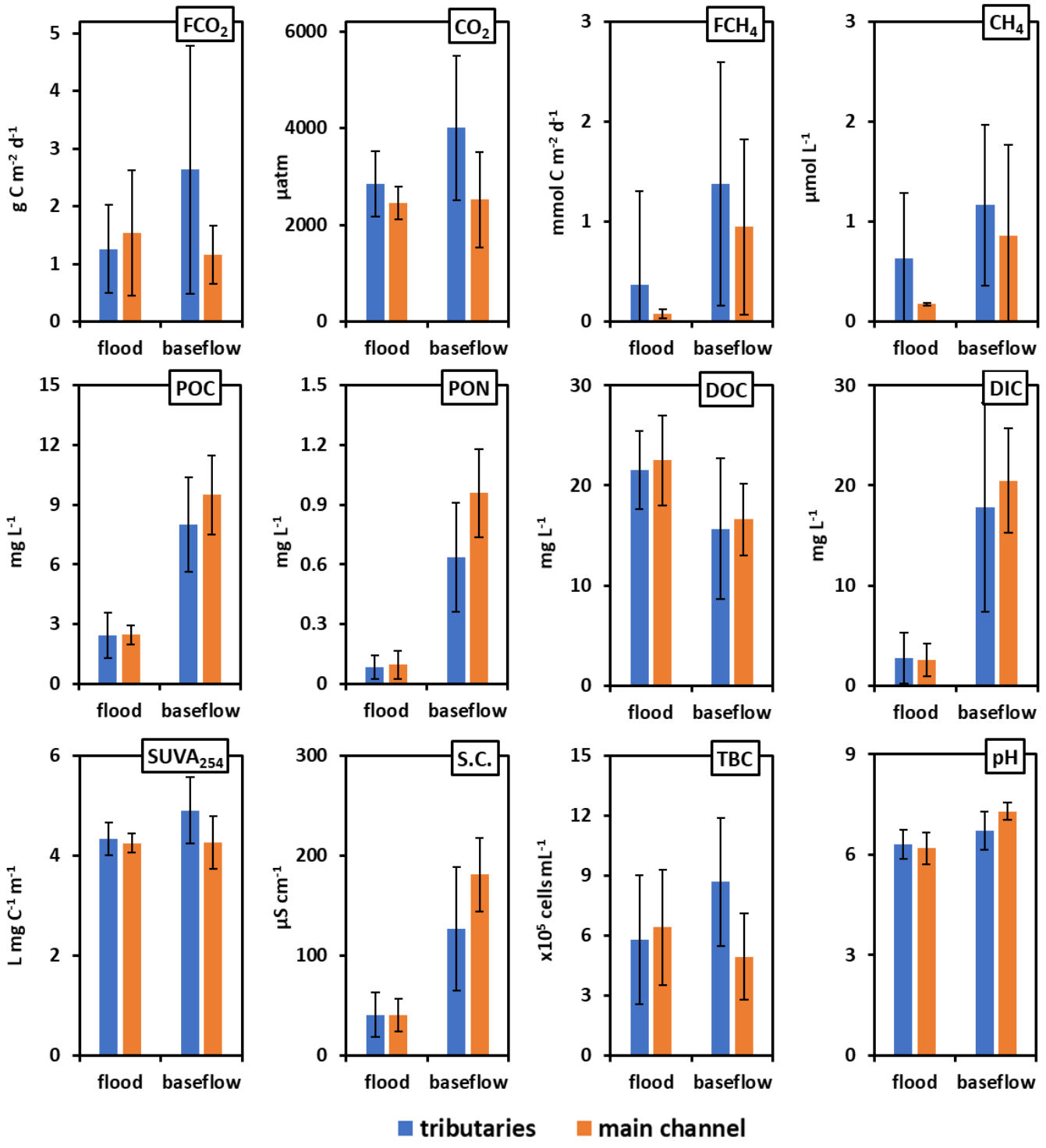


**Figure 3.** Mean (± s.d.) GHG concentration and chamber-measured fluxes ($FCO_2$), hydrochemical parameters, particulate organic carbon and nitrogen (POC and PON, respectively) and total bacteria count (TBC), in the main channel (orange column) and the tributaries (blue column) of the Ket River in spring flood and summer (early fall) baseflow.

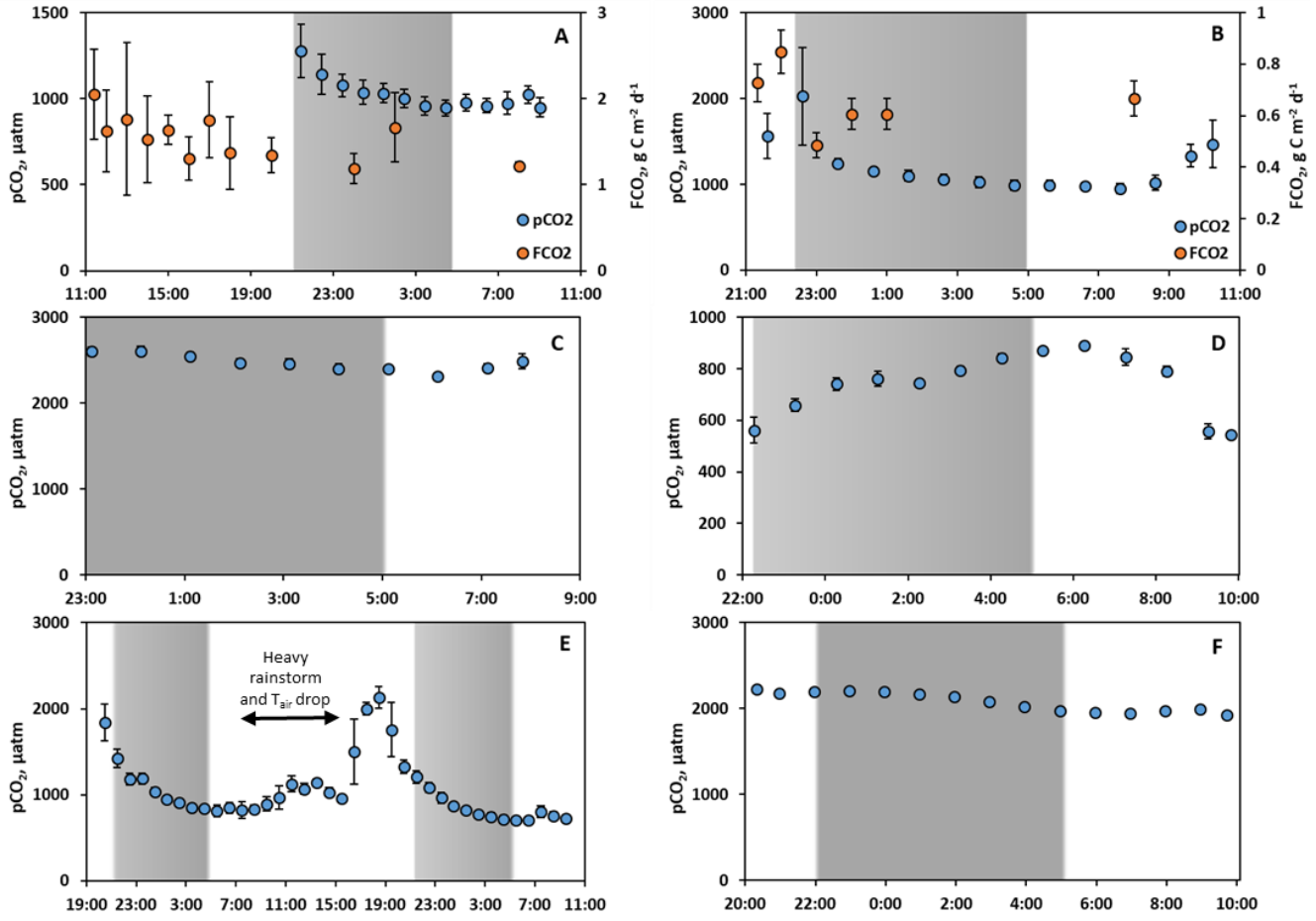


**Figure 4.** Continuous $pCO_2$ concentration (**A-F**, blue circles) and chamber-based fluxes (**A, B**) measured during spring flood period in tributaries (**A** Sochur No 3, **B** Lopatka No 8, **C** Derevyannaya No 12, **D** Ob river entrance, **E** Segondenka No 26) and in the Ket River main stem (middle course) near Stepanovka village (**F**) including night time measurements (shaded area). The measurement frequency was one per hour. Variations of water temperature were within the range of 0.3 to 0.6 °C and did not exhibit significant correlations with $pCO_2$ and $FCO_2$. Note that, for the small river Segondenka ($S_{watershed}$ = 472 km²), where the $CO_2$ peak was observed at 7 pm (**E**), there was quite heavy rainfall between 7 am and 3 pm.

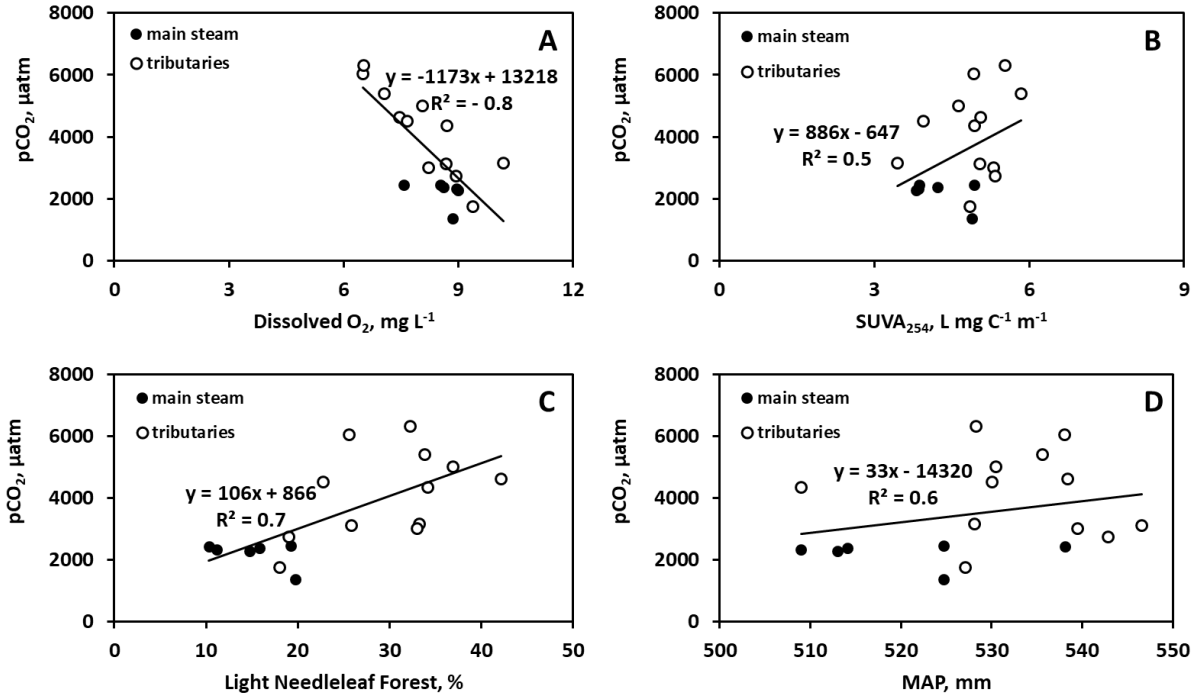


**Figure 5.** Significant ($p < 0.05$) control of dissolved oxygen (**A**), $SUVA_{254}$ (**B**), light needleleaf forest (**C**), and mean annual precipitation (**D**) on $CO_2$ concentration in the Ket River and tributaries during summer baseflow.